EFFECTS OF FRUCTAN SOURCE AND DEGREE OF POLYMERIZATION ON INTESTINAL BARRIER FUNCTION AND HISTOMORPHOLOGY CHARACTERISTICS IN OBESE C57BL/6 MICE

BY

KIMBERLY DANIELLE CEPHAS

THESIS

Submitted in partial fulfillment of the requirements
for the degree of Master of Science in Nutritional Sciences
in the Graduate College of the
University of Illinois at Urbana-Champaign, 2012

Urbana, Illinois

Master's Committee:

Associate Professor Kelly S. Swanson, Advisor
Professor Kelly A. Tappenden, Chair
Professor Emeritus George C. Fahey, Jr.

Abstract

Obesity is linked to increased intestinal permeability that may contribute to low grade inflammation. Fructan prebiotics have been demonstrated to increase intestinal resistance and decrease systemic inflammation. The objective of this study was to test the effects of prebiotics on intestinal permeability, morphology, and gene expression in an obese mouse model. Obese, 18-wk old, C57BL/6 mice were randomized to high-fat (45% of kcal) diets containing 5% cellulose, 10% cellulose, 10% short-chain fructooligosaccharides (scFOS) or 10% inulin and fed for 28 d. Distal ileum, cecum, and colon samples were collected for Ussing chamber, histomorphology, and qRT-PCR analyses. The effects of treatment were tested using the Mixed Models procedure of SAS. Among treatments, mice fed scFOS and inulin had greater ($p<0.05$) intestinal transmural resistance compared to mice fed 5% cellulose. MCT-1 expression was greater ($p<0.05$) in the distal colon of mice fed 10% cellulose compared to 10% inulin. ZO-1 expression was lower ($p<0.05$) in mice fed inulin compared to other treatments. Occludin mRNA abundance was lowest ($p<0.05$) in fructan sources compared to cellulose. When comparing 5% vs. 10% cellulose treatments using contrasts, 10% cellulose led to greater ($p<0.05$) intestinal crypt depth in all intestinal regions, except the distal colon. Mice fed 5% vs. 10% cellulose, however, had greater ($p<0.05$) ileal villus height: crypt depth ratio, ileal MUC2 mRNA abundance, proximal colon AMPK mRNA abundance, and occludin mRNA abundance in the proximal and distal colon regions. When comparing fructan vs. cellulose treatments using contrasts, fructans resulted in a greater ($p<0.05$) transmural resistance and crypt depth when all intestinal regions were combined. In contrast, fructan-fed mice had lower ($p<0.05$) mRNA abundance of ZO-1 and occludin when all intestinal regions were combined (Table 3.5). Fructan consumption resulted in lower ($p<0.05$) ileal MUC2 and occludin mRNA abundance, cecal occludin mRNA abundance, proximal colon MCT-1, ZO-1, AMPK, and occludin mRNA

abundance, and distal colon ZO-1, AMPK, and occludin mRNA abundance. Cecal AMPK mRNA abundance was greater ($p<0.05$) in fructan-fed compared to cellulose-fed mice. Pearson coefficient correlations indicated correlations between MCT-1 and distal colon ZO-1 ($r = 0.77$, $p<0.05$) and occludin mRNA abundance ($r = 0.66$, $p<0.05$). AMPK correlated with ZO-1 mRNA abundance ($r = > 0.60$, $p<0.05$) in all regions of the intestinal tissue of C57BL/6 mice. Lastly, ZO-1 mRNA abundance correlated with distal colon epithelial resistance ($r = 0.51$, $p<0.05$). Collectively, these data may suggest mechanisms by which equivalent quantities of fructan prebiotics and non-fermentable fibers affect intestinal barrier function.

Dedication

I dedicate this document to my heavenly Father who has been the ultimate guide and encouragement during my journey as a graduate student.

Acknowledgements

First and foremost, I thank Dr. Kelly Swanson. He has been an outstanding advisor. I truly admire the unlimited amount of patience and kindness he has shown me throughout my graduate career. He always has been positive, humble, humorous, and encouraging. I thank him for believing in me when I did not believe in myself!

I thank the Fahey and Swanson lab members, with whom I shared great times and much laughter, and who assisted me in making my Master's thesis a success.

I especially thank Katie Kerr, Ryan Grant, and Marcial Guevara for their patience in teaching me and for answering my 'million-and-one' questions.

I also thank Dr. George Fahey and Dr. Kelly Tappenden for their guidance and encouragement.

Lastly, I thank my family and friends for supporting me emotionally, mentally, and socially throughout my graduate career.

Table of Contents Page

Chapter 1

Introduction

According to the Centers for Disease Control and Prevention (CDC), in 2008, 34.4% of U.S. adults were overweight and 33.9% were obese. Furthermore, not one state in the U.S. had less than 15% of obese adults (which was the *Healthy People 2010* objective). The epidemic of obesity has plagued many Americans with co-morbidities such as hypertension, cardiovascular diseases, and type-2 diabetes. This condition is not only a detriment to quality of life, but also causes financial hardship. In 2008, those that were obese experienced $1,429 more in medical expenses than normal weight individuals due to obesity-induced co-morbidities (CDC Vital Signs, 2010). In addition, researchers found that obesity is also the predominant etiology of metabolic dysfunctions (Cani & Delzenne, 2009). Not only has excessive weight accumulated in the form of adipose tissue been shown to cause insulin resistance, hyperlipidemia, and low-grade inflammation, but also has been shown to change the intestinal microbiota negatively. Intestinal bacteria work symbiotically with the host to provide nutrients and promote gut health; however, a change in intestinal bacterial communities has been shown to cause declines in gut health, including increasing gut inflammation and intestinal barrier function deterioration. In an obese state, researchers have observed an increased colonization of Firmicutes and a decline in Bacteriodetes (Ley et al., 2006). This change in intestinal bacteria has not yet been linked to gut inflammation and intestinal barrier decline; however, it has been theorized that alterations in intestinal bacteria play a major role in the decline of gut health in an obese individual.

Maintenance of intestinal barrier function has been of great interest lately. The role of the intestinal barrier is highly significant and cannot be overlooked. In essence, it is the first line of defense against ingested noxious agents and hinders intestinal bacteria from entering systemic circulation, therefore preventing the fatal condition of sepsis (Groschwitz and Hogan, 2009).

In obese mouse models, this barrier has been compromised. Cani et al. (2009) reported decreased intestinal resistance in the jejunum of obese mice, which was associated with a change in intestinal bacteria and increased levels of systemic inflammation. That study also tested the effects of fructan prebiotics, which decreased systemic inflammation markers and intestinal barrier permeability. These indigestible carbohydrates, known as prebiotics, selectively stimulate beneficial bacteria in the gut of the host and have been shown to overcome the metabolic distress of obesity and produce a healthy microbiota in addition to restoring intestinal barrier function in the obese (Gibson and Roberfroid, 1995; Cani et al., 2009; Roberfroid et al., 2010). Fermentation of prebiotics not only lowers intra-luminal pH that decreases pathogen colonization within the gut and increases production of short-chain fatty acids, such as butyrate, which is the preferred energy source for colonocytes, but also has been found to decrease intestinal barrier permeability in obese mouse models.

The general objective of this research was to identify mechanisms by which the integrity of the intestinal architecture and barrier are improved via supplementation of prebiotics with varying fermentation characteristics in an obese mouse model.

Literature Cited

Cani, P. D., Possemiers, S., Van de Wiele, T., Guiot, Y., Everard, A., Rottier, O., Geurts, L., Naslain, D., Neyrinck, A., Lambert, D.M., Muccioli, G.G. & Delzenne, N.M. (2009). Changes in gut microbiota control inflammation in obese mice through a mechanism involving GLP-2-driven improvement of gut permeability. *Gut, 58*, 1091-1103.

Gibson, G. R., & Roberfroid, M. B. (1995). Dietary modulation of the human colonic microbiota: Introducing the concept of prebiotics. *J. Nutr., 125*, 1401-1412.

Groschwitz, K., & Hogan, S. (2009). Intestinal barrier function: Molecular regulation and disease pathogenesis. *J. Allergy Clin. Immunol., 124*, 3-20.

Ley, R., Turnbaugh, P., Klein, S., & Gordon, J. (2006). Human gut microbes associated with obesity. *Nature, 444*, 1022-1023.

Roberfroid, M., Gibson, G. R., Hoyles, L., McCartney, A. L., Rastall, R., Rowland, I., Wolvers, D., Watzl, B., Szajewska, H., Stahl, B., Guarner, F., Respondek, F., Whelan, K., Coxam, V., Davicco, M.J., Léotoing, L., Wittrant, Y., Delzenne, N.M., Cani, P.D., Neyrinck, A.M. & Meheust, A. (2010). Prebiotic effects: Metabolic and health benefits. *Brit. J. Nutr., 104*, S3-S51.

Vital signs: State-specific obesity prevalence among adults---United states, 2009. (2010, August 3). Retrieved December 30, 2011, from CDC: Centers for Disease Control and Prevention: http://www.cdc.gov.

Chapter 2

Literature review

Intestinal barrier function

The selective permeability of the intestinal barrier is an important component of gastrointestinal function. It not only is comprised of a single-cellular epithelial layer that is conjoined by the primary supports of tight junction (TJ) adhesions, but also consists of a mucus layer and associated immune cells (Groschwitz and Hogan, 2009; Rescigno, 2011). However, the physical restrictions applied by the TJ (lateral spacing between epithelial cells) may warrant the greatest attention in maintaining the integrity of the barrier and the health of the host. The TJ functions to prevent the paracellular transport of intraluminal toxins, intestinal microflora, and foreign antigens from invading the lamina propria, portal circulation, and, eventually the systemic circulation. Paracellular transport is the passive diffusion of substrates through the intercellular space between adjacent epithelial cells. Tight junction proteins regulate the permeability of the paracellular space at the lateral membrane of each epithelial cell (Groschwitz and Hogan, 2009). Intestinal barrier regulation is accomplished through TJ protein-protein interactions and intracellular anchoring of TJ proteins to the actin cytoskeleton of the intestinal cells (Groschwitz and Hogan, 2009).

There are three main TJ membrane proteins involved in the maintenance of the intestinal barrier: claudins, occludins, and zonula occludens (ZO). Junctional adhesion membrane (JAM) proteins have been less studied, but are also important in the maintenance of the intestinal barrier. Claudins contain hydrophobic transmembrane domains anchored by ZO intracellularly, and contain hydrophilic extracellular loops, that extend into the paracellular space (Van Itallie and Anderson, 2006). These loops are vital in the formation of ion-selective channels within the TJ complex. Furuse et al. (2002) demonstrated the importance of claudins, with the claudin-1

mutation (claudin-1 knockout mice) being fatal due to substantial transepidermal water loss. Occludin functions by interacting with ZO to adhere itself to the actin cytoskeleton of each epithelial cell (Furuse et al., 1994; Mitic et al., 2000). The hydrophilic domains of the occludin protein extend into the paracellular pathway to aid in selective transport. ZO-1, -2, and -3 form dense protein structures, known as cytoplasmic plaques in conjunction with other TJ adhesions (Groschwitz and Hogan, 2009). The interaction of ZO adhesions with JAM proteins is vital to the function of the TJ and cell-to-cell border. The crucial role of ZO proteins has been shown in ZO-1-deficient and ZO-2-deficient mouse embryos, which contained apoptic or necrotic cells in the notochord and neural tube, decreased angiogenesis due to vascular defects, and increased permeability in the apical junctions of embryonic cells. These finding were consistent with arrest of the embryos in early gastrulation (Katsuno et al., 2008; Xu et al., 2008). Laukoetter et al. (2007) reported that disruptions in siRNA-mediated knockdowns of JAM-A proteins in human SK-C015 colonic monolayers reduced ($P<0.05$) transepithelial resistance (TER) by 60% compared to controls. Furthermore, these researchers reported that JAM-A knockout mice suffered from increased dextran permeability, which was consistent with reduced TER, enhanced mucosal permeability and increased susceptibility to colitis, further indicating the importance of JAM proteins as structural adhesions in the intestinal barrier (Laukoetter et al., 2007). Researchers also have reported an extended role of ZO TJ proteins. Itoh et al. (1999) reported increased localization of ZO-1, -2, and -3 proteins at the TJ of intestinal epithelial cells in occludin- deficient mice. Immunoblotting procedures identified the interaction of ZO-1, -2, and -3 bound to the C-terminus of claudin TJ proteins of these mice, which may indicate increased expression of ZO adhesions in order to maintain homeostasis of the epithelial barrier (Itoh et al., 1999).

The contributions of each TJ protein serve an extraordinary function in preventing a leaky intestinal barrier. Maintaining the epithelial barrier decreases the host's risk of bacteremia, endotoxemia [high levels of translocated bacterial lipopolysaccharides (LPS) from the gut to systemic circulation], and the uptake of intraluminal toxins and other osmotic contents into the systemic circulation. Therefore, the regulation of the intestinal barrier function is extremely important for health.

Intestinal barrier dysfunction and its consequences

There are conditions that can cause detrimental alterations to the barrier by inducing rearrangement and deterioration of the proteins composing the TJ complex, leading to intestinal and metabolic complications. A reduced epithelial barrier has been shown in several disease states, such as inflammatory bowel disease (IBD), sepsis, metabolic syndrome, and allergic responses, such as celiac disease. The symptoms of these diseases suggest intestinal barrier deterioration and associated consequences of dysbiosis, the mechanisms of which are discussed below.

The disruption of the intestinal barrier can involve the TJ and the distortion of the cellular components of the barrier as well, including epithelial cell hypertrophy and apoptosis and villus atrophy (Song et al., 2009; John et al., 2011). Disruption of the epithelial barrier increases intestinal permeability and can yield explicit symptoms of osmotic diarrhea through paracellular and transcellular transport of solutes into the intestinal lumen, as seen in IBD patients [inclusive of ulcerative colitis (UC) and Crohn's disease (CD)], with mild to severe intestinal inflammation. Mild ileocolonic inflammation, as generated in a $TNF^{(+/\Delta ARE)}$ rodent model, which displays chronic to mild ileocolitis due to over-expression of TNF-α, was reported to result in decreased epithelial bicarbonate secretion and depression of fluid absorption within the ileum; these

findings were attributed to intestinal barrier breakdown (Xiao et al., 2011). It is speculated that the loss of gut barrier function is involved in the pathogenesis of multiple organ dysfunction syndrome (MODS) (Ammori et al., 1999; Velasco, 2006). Such patients were found to have high serum diamine oxidase (DAO) concentrations, which are released by damaged mucosal epithelial cells, endotoxemia, and a pronounced reduction in TER, all of which correlate strongly with intestinal barrier dysfunction (Zhang et al., 2010). MODS patients who underwent continuous venovenous hemofiltration for 24 h had a reduction ($p<0.05$) in serum DAO and increased ($p<0.05$) TER compared to 0 h. Gut barrier loss was attributed to downregulation and reorganization of TJ adhesions. Specifically, intestinal occludin and ZO-1 protein levels were 50% lower ($p<0.01$) in MODS patients compared to healthy controls (Zhang et al., 2010).

Intestinal bacteria appear to have an important role in the pathogenesis of intestinal barrier dysfunction. A correlation between intestinal barrier decline and specific microbiota has yet to be discovered. However, certain microbial species have been linked to IBD and it is known that during active IBD, intestinal architectural and TJ complexes undergo structural changes. Frank et al. (2007) reported that small bowel mucosal biopsies of IBD patients had decreased ($p<0.001$) populations of *Lachnospiraceae* (subgroup of *Firmicutes*) by more than 300-fold and *Bacteroidetes* by 50-fold and increased ($p<0.001$) *Proteobacteria* and *Bacillus* (subgroup of *Firmicutes)* compared to non-IBD patients. Frank et al. (2011) did not report a difference in *Enterobacteriaceae* (phyla *Proteobacteria*) populations in IBD patients vs. controls, yet Kotlowski et al. (2007) reported that *E. coli* (family *Enterobacteriaceae*) were 3 to 4 log units greater ($p<0.05$) in IBD patients with increased ($p=0.04$) pathogenic B2+D phylogenetic groups of *E. coli* (*E. coli* phylogenic groups B2 and D are virulent groups) compared to controls. *E. coli* is classified as a gram-negative bacterium and has been implicated

in endotoxemia (Raetz and Whitfield, 2002). Bloom et al. (2011) also reported the involvement of specific commensal bacteria in the development of IBD. Bacterial members of the genus *Bacteroides*, specifically *Bacteroides vulgates* and *Bacteroides thetaiotaomicron*, were reported to cause severe UC in conventionalized germ-free dnKO mice (mice contain defects in IL-10 and TGFβ anti-inflammatory pathways) (Bloom et al., 2011). This study also reported that the presence of Firmicutes (families including *Lactobacillaceae, Bacillaceae* and *Lachnospriaceae*) did not generate colitis in conventionalized germ-free dnKO mice. Zeissig et al. (2007) used freeze fracture electron microscopy to report a decline ($p<0.001$) in TJ adhesions (4.7 TJ strands per 1000 nm single-strand length) at the surface of the sigmoid colon during active CD compared to healthy controls (7.2 TJ strands per 1000 nm single-strand length) and reduced ($p<0.001$) TJ adhesions within the crypt compared to controls (4.4 TJ strands and 7 TJ strands per 1000 nm single-strand length, respectively). Furthermore, these researchers reported decreased ($p<0.01$) transmural impedance among active CD patients (23 $\Omega*cm^2$ compared to 39 $\Omega*cm^2$ in controls). Proinflammatory mediators, TNF-α and IFN-γ, which are associated with LPS-mediated cytokine release, have been found to deteriorate TJ architecture by decreasing claudin expression and ZO-1 redistribution in IBD patients (Zeissig et al., 2007; Capaldo and Nusrat, 2009). Collectively, these findings suggest a sequence of events leading to declining intestinal barrier function. Disruption of the intestinal barrier is associated with endotoxemia in IBD patients. Approximately 88% of UC patients and 94% of CD patients have been reported to have systemic endotoxemia (Gardiner et al., 1995; Zeissig et al., 2007). Endotoxemia causes an uncontrolled immunological response leading to secretion of proinflammatory cytokines, organ dysfunction, growth failure in children, and in 60% of severe sepsis patients, death (Pasternak et al., 2010; Krzystek-Korpacka et al., 2011).

The endotoxin, LPS, is found within the cell wall of gram-negative bacteria, such as *E. coli*. For every *E. coli* cell present within the human gut, there is 10^6 lipid A residues (~80% of the bacterial cell wall), which is the active endotoxin component of LPS (Raetz and Whitfield, 2002; Taniguchi et al., 2009; Laugerette et al., 2010). It is pertinent to note that within the gastrointestinal tract of a healthy human, there is 0.1 mg of LPS present, which may not cause any harm to the host; however, this value varies based on one's diet, weight, lifestyle, and overall health (Raetz and Whitfield, 2002; Taniguchi et al., 2009). Lipopolysaccharides elicit a proinflammatory immunological response via pattern-recognition receptors called toll-like receptors (TLR), that are found on macrophages, dendritic cells, intestinal epithelial cells, and other antigen-presenting cells (Taniguchi et al., 2009; Khoo et al., 2011).

Another primary factor thought to lead to increased intestinal barrier permeability is diet. High consumption of alcohol and dietary fats, such as palmitic acid (C16:0) and oleic acid (C18:1), have been evaluated for their effects on the integrity of the intestinal barrier. Researchers have shown that increased alcohol intake can reduce intestinal barrier function through downregulation and reorganization of TJ adhesions. Zhong et al. (2010) reported that a daily intake of ethanol at 38% of total caloric intake by C57BL/6 mice decreased apical-lateral dispersal of ileal ZO-1 and occludin at the TJ complex. In congruence with TJ function, it was also reported that the absorption of FITC-dextran with a molecular weight of 4,000 (FD-4) within the ileum was higher ($p<0.05$) in alcohol-fed mice (~3 μg/cm/min) compared to controls (1 μg/cm/min). This increased ileal permeability also was associated with elevated ($p<0.05$) plasma LPS concentrations in the alcohol-fed mice (0.5 EU/ml) compared to controls (0.2 EU/ml), which suggests that high alcohol consumption causes the disarray of TJ adhesions, increased intestinal permeability, and leakage of bacterial endotoxins into systemic circulation

(Zhong et al., 2010). Excessive alcohol intake is also thought to cause an overgrowth of gram-negative bacteria and LPS flux in the gut, possibly contributing to these changes.

Excessive caloric intake in the form of dietary lipids was evaluated by Suzuki and Hara (2010) in lean Long Evans Tokushima Otsuka (LETO) and obese Otsuka Long Evans Tokushima Fatty (OLETF) rats. The results of this study concluded that intestinal permeability measured via Cr-EDTA excretion in urine was higher ($p<0.01$) in LETO and OLETF rats consuming a high-fat diet (average 4.5% urinary Cr-EDTA, 300 g/kg; 7% soybean oil, 23% lard) compared to a standard diet (average 2.85% urinary Cr-EDTA, 70 g/kg; soybean oil only). In the small intestinal mucosa cell fractionations of both OLETF and LETO rats consuming a high-fat diet vs. standard fed rats, a reduced expression of TJ proteins, shown as the area under the curve (AU) was found, such as claudin-1 (average 0.475 AU vs. 1.25 AU), claudin-3 (average 1.02 AU vs. 1.5 AU) and JAM-1 (average 0.9 AU vs. 1.1 AU) (Suzuki and Hara, 2010). Furthermore, plasma TNF-α concentrations were 3 times higher ($p<0.05$) in the OLETF rats consuming a high-fat diet compared to OLETF rats consuming the standard chow diet and LETO rats fed the high-fat or standard chow diets. It is well documented that high-fat diets stimulate TLR4 receptors in a similar manner as lipid-containing bacterial endotoxins. Suganami et al. (2007) reported that TLR4 knockout murine peritoneal macrophages treated with palmitate attenuated ($p<0.01$) TNF-α mRNA expression. Furthermore, DNA microarray analysis of RAW264 macrophages (murine macrophage cell lines) incubated with palmitate or LPS showed up-regulation of TNF-α and genes in the NF-κB pathway, such as NF-κB1 (p50) and RelA (p65); therefore, the conclusion was made that palmitate and LPS use the NF-κB pathway as a common pathway for cytokine secretion (Suganami et al., 2007). Cytokine release, in turn, can lead to

disorganization of the TJ proteins at the apical-lateral membrane causing increased intestinal permeability (Adams et al., 1993; Shi et al., 2006).

In addition to studying total dietary fat concentrations in inflammatory processes, others have assessed the involvement of specific fatty acids. The lipid composition of animal fats, which are thought to be associated with inflammatory processes, consist of 26.6% palmitic acid and 43.1% oleic acid (Zhao et al., 2005). Rockett et al. (2010) reported that incubation of B cells with 50 mM of palmitate for 48 h increased ($p<0.05$) apoptosis by 3-fold compared to a BSA control. Aspenstrom-Fagerlund et al. (2007) demonstrated that Caco-2 cells exposed to 15 or 30 mM of oleic acid between 30 to 90 min caused cytotoxicity [as measured by apical leakage of lactate dehydrogenase (LDH)], increased ($p<0.05$) ^{12}C-mannitol absorption (~ 2% absorption), which measures paracellular permeability, and decreased ($p<0.05$) transepithelial electrical resistance (TEER) compared to controls (0% absorption of 12C-mannitol and 117% relative TEER, respectively); 5 mM of oleic acid exposure from 30 to 90 min, however, had no effect on the absorption of ^{12}C-mannitol in these monolayers, indicating the deterioration of the barrier in a dose-and time-dependent manner. These reports suggest that the dietary fatty acids ingested are significant in regulating the expression of TJ proteins and influencing intestinal permeability, possibly through cytokine-mediated processes (Rockett et al., 2010). Further assessment of the fatty acid composition has shown that increased intake of omega-6 (n-6) fatty acid composition sources (e.g., animal fats, meats, and corn oil), commonly found in the Western diet, leads to the generation of prostaglandins PGE_2, PGI_2, and TXA_2 derived from arachidonic acid (AA), which employs a proinflammatory effect (Russo, 2009). Therefore, an imbalance of n-6:n-3 of 20:1, which is commonly found in the Western diet, has been implicated in the generation of such diseases as cardiovascular disease due to increased oxidation of lipoproteins and proaggregate

compounds (Simopoulos, 2002; 2006). An imbalance of n-6:n-3 also has been shown to be involved in the decline of the intestinal barrier function in gastrointestinal diseases such as IBD. Usami et al. (2003) reported independent incubation of 10 to 100 μmol of eicosapentaenoic acid (EPA), an n-3 fatty acid, decreased ($p<0.01$) TEER (0.75 vs. 0.95 of controls) and increased ($p<0.05$) paracellular transport in Caco-2 cell monolayers (2% permeability to fluorescein sulfonic acid [FS] vs. 1.3% in controls). Similarly, γ-linolenic acid (n-6) also was reported to decrease ($p<0.001$) Caco-2 cell monolayer paracellular permeability in a dose-dependent manner (8% FS permeability vs. 1% FS permeability in controls) and decrease ($p<0.001$) TEER (0.5% compared to 1% in controls) (Usami et al., 2003). This evidence shows the independent actions of n-3 and n-6 on paracellular permeability. In contrast, T84 human intestinal epithelial cells and a pancreatic lipase, used to facilitate deterioration of the intestinal barrier, incubated with a fat blend of n-6 (13.05 w%) and n-3 (1.87 w%) at 100 μM concentration was reported to have higher ($p<0.001$) TER and lower ($p<0.001$) IL-4 secretion compared to controls incubated with the pancreatic lipase only (Willemsen et al., 2008). This report suggests the association of n-6 and n-3 together can reduce intestinal barrier damage and inflammation.

Recent evidence also has shown an influence of high-fat diets on intestinal microbial communities, which may lead to increased systemic LPS and inflammation in obese models. Diet-induced obese-prone (DIO-P) rats fed a high-fat diet have been shown to have altered intestinal bacterial populations when compared to DIO-P rats fed a low-fat diet and diet-induced obese-resistent (DIO-R) rats fed a high-fat diet. For instance, cecal *Bacteroidales* and *Clostridiales* were increased ($p<0.01$) in DIO-P and DIO-R rats fed a high-fat diet (31% and 23% of total bacteria, respectively) compared to DIO-P and DIO-R rats fed a low-fat diet (26% and 11% of total bacteria, respectively) (Barbier de La Serre et al., 2010). These findings were

accompanied by elevated ($p<0.05$) plasma LPS (10 EU/ml) in DIO-P rodents fed a high-fat diet compared to lean-fed and DIO-R rodents fed a high-fat diet (0.5 EU/ml) (Barbier de La Serre et al., 2010). In healthy male subjects, Erridge et al. (2007) reported that a high-fat diet increased ($p=0.05$) plasma endotoxins, from 8.2 pg/ml (baseline, before meal) to 12.2 pg/ml (after high-fat meal). Furthermore, an *in vitro* challenge of 1000 pg/ml LPS to human aortic endothelial cells was reported to elevate ($p<0.05$) IL-8 and TNF-α 3-fold compared to cells which received 0 pg/ml LPS. These data indicate an association between high-fat diet-induced plasma endotoxin increases and inflammatory response (Erridge et al., 2007).

Although various changes in dietary intake and intestinal bacteria may lead to increased permeability, the transition to disease ultimately involves proinflammatory cytokine release and deterioration of TJ architecture. The association between cytotoxicity and TJ dysfunction has been demonstrated by several research groups. Adams et al. (1993) demonstrated that T84 human colonic cell lines incubated with IFN-γ in a dose-dependent manner (0, 10, 100, and 1000 U/ml), decreased ($p<0.05$) monolayer relative resistance from 1.3 (0 U/ml IFN-γ) to less than 0.6 (1000 U/ml IFN-γ) within 72 h of exposure. Ma et al. (2004) incubated Caco-2 cell monolayers with TNF-α and reported a decrease ($p<0.01$) in epithelial resistance (< 350 $\Omega*cm^2$) in those cells compared to controls without TNF-α (550 $\Omega*cm^2$). Peng et al. (2009) evaluated Caco-2 cell monolayers undergoing calcium switch procedures via removal and introduction of calcium into the cell culture medium to understand the mechanism of proinflammatory markers. Calcium is an essential mineral to the maintenance of the TJ; therefore, its removal from the medium led to the redistribution of TJ proteins, ZO-1 and occludin, from the apical-lateral membrane to the cytoplasm, which to increased cell monolayer permeability (Peng et al., 2009). These data concluded that immediate disruption to the TJ was due to the translocation of TJ adhesions to the

cytoplasm. Youakim and Ahdieh (1999) and Bruewer et al. (2003) reported that IFN-γ and TNF-α decreased epithelial barrier TJ proteins by reducing protein expression and localization to the apical-lateral membrane, further clarifying the mechanism of action involved in the increased permeability of the epithelial layer. The mechanistic action of TNF-α on permeability is thought to function through the activation of the NF-κB signal transduction pathway, further leading to reorganization of TJ proteins and altered epithelial resistance due to cytokine-induced deterioration (Youakim and Ahdieh, 1999; Bruewer et al., 2003; Barbier de La Serre et al., 2010). Indeed, through pharmacological inhibition of NF-κB, investigators have discovered a reduction in intestinal barrier permeability and increased TJ stability. Based on these findings, it is evident that long-term exposure of multiple proinflammatory cytokines can cause dysfunction of the epithelial barrier through TJ remodeling (Ammori et al., 1999; Zhang et al., 2010).

Intestinal barrier dysfunction in obesity

Researchers have found several sources of the proinflammatory markers produced in obesity, including both adipose and intestinal tissues. This inflammation further contributes to the metabolic dysfunction and disruption of the intestinal barrier. Not only does the metabolic dysfunction of hyperplastic adipocytes include insulin resistance, but also enlarged adipocytes have been implicated in being the predominant source of inflammation in obese individuals (Maury and Brichard, 2010). Ye et al. (2007) reported a 70% reduction ($p<0.001$) of the pO_2 in the epidiymal fat pads of *ob/ob* (leptin-deficient) mice compared to lean controls. This difference in pO_2 indicates the presence of hypoxia in the adipose tissue of these obese mice (Ye et al., 2007). Furthermore, due to apoptosis and necrosis of adipocytes, secretion of proinflammatory cytokines, such as TNF-α and IL-6, from the adipose tissue was higher ($p<0.001$, $p<0.05$

respectively) in the *ob/ob* mice (10- and 5-fold, respectively) compared to lean controls (1- and 1-fold, respectively) (Ye et al., 2007).

Hypertropic adipocytes also secrete chemokines that recruit macrophages to eradicate cellular fragments after adipocyte apoptosis (Virtue and Vidal-Puig, 2010). Weisberg et al. (2003) identified macrophages by immunohistochemical staining for the antigen F4/80, which is an indicator of mature macrophages, within adipose tissue of lean and obese mice. The clustering of macrophages in the adipose tissue of the lean mouse model was minor and scattered throughout the tissue (Weisberg et al., 2003). Alternatively, macrophages in obese rodents were repeatedly found amassed in a crown-like structure around necrotic adipocytes.

The diverse community of intestinal bacteria within the human gut has been known for many years to possess metabolic capabilities not present in the host. The bacterial microbiome is an additional 'organ' capable of metabolic functions, which are vital to the host. Due to high-throughput sequencing techniques, the global characterization and study of gut microbes has been identified. Saccharolytic activity by intestinal bacteria can yield fermentative end-products [e.g., short-chain fatty acids (SCFA)] that can be beneficial to the host that would have been otherwise lost to fecal excretion. However, in understanding the metabolic capabilities of intestinal bacteria, Backhed et al. (2004) reported that germ-free mice had increased ($p<0.01$) total body fat (57%) and epididymal fat weight (61%) after conventionalization (inoculation of unfractionated microbiota from ceca of control mice). This information demonstrates the importance of intestinal bacteria in energy harvest and the deposit of fat in subcutaneous stores.

Researchers have tried to identify the potential role intestinal bacteria have in the metabolic dysfunction of obesity. Creely et al. (2006) reported metabolic endotoxemia to be greater ($p<0.0001$) in type 2 diabetes mellitus patients (5.5 log EU/ml) compared to non-diabetic

patients (3.1 log EU/ml). More specifically, endotoxin levels were noted to be higher ($p=0.0031$) in type 2 diabetic individuals with a BMI greater than 30; TNF-α serum levels were also 2.5 times higher ($p=0.00685$) in these patients compared to non-diabetic controls with a BMI less than 30 (Creely et al., 2006). Researchers have debated whether the intestine of obese individuals contains variations in intestinal microbiota, with initial studies focused on the Bacteroidetes and Firmicutes phyla. Ley et al. (2005) reported a 50% decrease ($p<0.05$) in Bacteriodetes in *ob/ob* mice and an equal increase ($p<0.05$) in Firmicutes compared to lean controls. To understand if intestinal bacteria were changing due to the diet or the obese state, Ley et al. (2006) evaluated fecal samples of 12 obese human subjects on a fat-restricted or carbohydrate-restricted diet for 1 yr. Before nutritional intervention, feces of obese subjects contained more ($p=0.002$) Firmicutes (90% of total rRNA gene sequences) and fewer ($p<0.001$) Bacteroidetes (< 5% of total rRNA gene sequences) compared to lean controls. As the subjects decreased in body weight, Bacteroidetes (70% of total rRNA gene sequences) increased ($p<0.001$) and Firmicutes (25% of total rRNA gene sequences) decreased ($p=0.002$); these findings were independent of diet composition (Ley et al., 2006). Strong correlations ($r^2 = 0.5 - 0.8$) were noted between weight reduction and increased ($p<0.05$) Bacteriodetes. These data may indicate an alternation of intestinal bacteria based on weight (obese state) that is irrespective of diet type. Zhang et al. (2009) also reported evidence in support of microbiota change in an obese model. Fecal Prevotellaceae (phylum Bacteroidetes) were higher ($p=0.040$) in morbidly obese (BMI > 35) individuals (5% of total rRNA gene sequences) compared to normal weight controls (0% of total rRNA gene sequences) (Zhang et al., 2009).

Current evidence suggests a connection between changing microbial communities in the obese and increased intestinal permeability and risk of endotoxemia. Barbier de La Serre et al.

(2010) reported a decrease in total bacterial 16S rRNA gene copies per gram wet weight in DIO-P (3.5×10^7) rats compared to DIO-R rats (5.0×10^7). Enterobacteriales populations were > 2 fold higher ($p<0.05$) in DIO-P compared to DIO-R rats independent of diet composition. In addition, plasma LPS concentrations were 9 times greater in the DIO-P mice fed a high-fat, compared to DIO-P and DIO-R rats on a high-fat diet and low-fat fed Sprague-Dawley rat controls (Barbier de La Serre et al., 2010). DIO-P rats also had greater ($p<0.001$) intestinal permeability (> 1 ug/ml dextran) compared to DIO-R rats (< 0.5 ug/ml). Intestinal permeability was attributed to translocation of the TJ protein, occludin, from the ileal TJ to the cytoplasm of the enterocytes. DIO-P rats contained greater ($p<0.001$) occludin proteins (15%; measured as the percentage of positive pixels in confocal images after immunochemical staining of designated tissue) in the ileal cytoplasm compared to DIO-R (5%). Collectively, this evidence suggests a strong relationship between a change in cecal intestinal bacteria, increased intestinal permeability, and endotoxemia. To assess whether high-fat diets increase LPS translocation to systemic circulation, Cani et al. (2007) gavaged C57BL/6 mice with LPS-oil or LPS-water mixtures. The oil resulted in higher LPS ($p<0.05$) absorption (4 EU/ml) compared to in LPS-water controls (-2 EU/ml plasma LPS) within 30 min of treatment. In support of this work, Brun et al. (2007) reported that *ob/ob* and *db/db* (leptin-receptor deficient) obese mice had decreased ($p<0.05$) TER (25 $\Omega*cm^2$ and 32 $\Omega*cm^2$, respectively) compared to the wild-type control mice (44 $\Omega*cm^2$). These findings were associated with elevated ($p<0.05$) serum IL-6 (3 ng/ml, 7.5 ng/ml, 2 ng/ml in *ob/ob*, *db/db* and control, respectively), IFN-γ (6.5 ng/ml, 31.5 ng/ml, and 6.5 ng/ml, respectively) and TNF-α (60 ng/ml, 60.5 ng/ml, and 31.5 ng/ml, respectively). Furthermore, serum endotoxin concentrations were 3 times greater ($p<0.02$) in *db/db* mice compared to controls (Brun et al., 2007). These findings were attributed to TJ reorganization of

occludin and ZO-1 in the ileum. The authors concluded that *ob/ob* and *db/db* intestinal permeability and subsequent anomalies were attributed to the obese phenotype of these rodents rather than the lack of leptin function. These studies demonstrate an inflammatory state in obese models, possibly due to intestinal bacteria changes and endotoxemia.

Benefits of intestinal bacteria and fructan-based prebiotics

The bacterial ecosystem of the human gut contains over 500 microbial species in a quantity 10 times greater than the number of eukaryotic cells that make up the human body (Guarner and Malagelada, 2003). The colon contains the highest concentrations of bacterial cells, ranging from 10^{11} to 10^{12} bacterial cells/g of intraluminal contents (Gibson and Roberfroid, 1995). Intestinal bacteria share a symbiotic relationship with humans, providing benefits such as salvaging energy from undigested carbohydrates, inhibition of pathogen colonization within the host gut, biosynthesis of vitamins, and by decreasing blood ammonia concentrations (Gibson and Roberfroid, 1995). Gnotobiotic rodents have been used recently to demonstrate metabolic functions of intestinal bacteria. Reikvam et al. (2011) depleted intestinal microbiota in conventional mice to understand the biological role of intestinal bacteria. In that study, mice were gavaged with amphotericin-B every 12 h for 3 d, followed by supplementation of 1 g/L of ampicillin into their drinking water and an antibiotic mixture of vancomycin, neomycin, metronidazol, and amphotericin-B every 12 h for 17 d (Reikvam et al., 2011). This treatment resulted in < 1 bacterial cfu/mg of feces, which was associated with hypoplastic Peyer's patches and spleen, hyperplastic ceca, and reduced epithelial proliferation in the mice (Reikvam et al., 2011). In addition to the effects of intestinal microbiota on gastrointestinal health and development, previous studies have found that the absence of intestinal bacteria also has effects on all organ systems and metabolic functions in the host. For instance, smaller liver, reduced

total blood volume and cardiac output, thinner alveolar and capsule wall in the lungs, and decreased iodine uptake by the thyroid gland were noted (Smith et al., 2007). In addition, intestinal morphology and immune function are altered. Studies have shown that germ-free models have cecal walls and mucosa that are thinner, decreased intestinal IgA, and increased susceptibility to pathogenic bacteria, such as *Shigella flexneri* and *Listeria* (Smith et al., 2007).

Traditionally, bifidobacteria and lactobacilli were thought to be among the predominant beneficial bacteria within the human gut and have the greatest potential in metabolic capabilities of the host upon stimulation (Gibson and Roberfroid, 1995; Zhu et al., 2010). A large body of research has demonstrated the benefits of indigestible carbohydrates known as prebiotics, to selectively stimulate the growth and activity of commensal bacteria that in turn lead to health benefits in the host. As a probiotic bolus, *Lactobacillus* has been found to alleviate endotoxemia and reduce the pathology of alcoholic liver injury in Wistars rats consuming a corn oil and alcohol treatment (Nanji et al., 1994). Langlands et al. (2004) reported that the supplementation of 7.5 g of oligofructose and 7.5 g of inulin (total 15 g/d) tended to increase ($p=0.059$) bifidobacteria in the proximal colon of mucosal biopsies of healthy adults (6.3 CFU/g mucosa) compared to controls (5.3 CFU/g mucosa). Similarly, distal colon bifidobacteria of oligofructose- and inulin-supplemented participants were greater (6.4 CFU/g mucosa, $p<0.05$) than those without prebiotic supplementation (5.2 CFU/g mucosa) (Langlands et al., 2004). Increased colonization of bifidobacteria has been associated with a reduction in pathogenic microflora, strengthened intestinal immune function via increased intestinal IgA plasmacytes, and reduced colon carcinogenesis and risk of bowel diseases (Mitsuoka, 1990; Grizard and Barthomeuf, 1999).

Cani et al. (2007) reported that *Bifidobacterium* spp. were lower ($p<0.05$) in the ceca of *ob/ob* mice fed a high-fat diet (less than 7.5 log bacterial cells/g cecal contents) compared to *ob/ob* mice fed a control diet (greater than 8.5 log bacterial cells/g cecal contents). In that study, plasma LPS was negatively correlated ($r = -0.41$, $p=0.025$) with cecal bifidobacteria, suggesting a protective role offered by bifidobacteria against endotoxemia (Cani et al., 2007). Furthermore, Cani et al. (2009) reported a reduction ($p<0.05$) in plasma TNF-α levels of *ob/ob* mice (50 pg/ml) fed a diet containing 10% oligofructose compared to *ob/ob* controls (200 pg/ml) fed a standard chow diet.

While many dietary ingredients may possess some degree of prebiotic activity, fructans have been the most heavily studied and shown to promote health by promoting a "healthier" colonic microbiota. Fructans are primarily composed of β-(2 → 1) fructosyl-fructose linkages and are naturally found in chicory root, Jerusalem artichokes, onions, bananas, and wheat products (Roberfroid, 2005). The nomenclature of fructans is largely based on chain length. Inulin has the highest degree of polymerization (DP), which is between 10 and 60. Oligofructose is a partially hydrolyzed product of long-chained inulin and contains a DP less than 10 (Roberfroid et al., 1998; Hernot et al., 2009). Short-chain fructooligosaccharides (scFOS) have an average DP of 3 – 6 and are most often synthesized from sucrose (Roberfroid et al., 2010). Depending on chain length, fructans are capable of exerting beneficial effects on the host through selective increase of beneficial microflora in different regions of the gut, ranging from the distal ileum to the distal colon.

Fermentative by-products produced by intestinal microbiota are dependent upon the substrate fermented but, in general, end-products include hydrogen and carbon dioxide gases, ammonia, phenols, indoles, amines, SCFA, and other organic acids (Macfarlane, 1991). The

principal energy source derived from fermentation that is available to the host is in the form of SCFA, mainly acetate, propionate, and butyrate (Macfarlane and Macfarlane, 2003). Through the salvaging of this energy from dietary fibers, SCFA comprise 5-15% of human's total caloric requirements (Hamer et al., 2008). Large intestinal contents of sudden death victims have been reported to contain concentrations of acetate: propionate: butyrate at 57:22:21 mmol/kg (Macfarlane and Macfarlane, 2003). However, because substrate availability and fermentative capacity is highest in the proximal colon, these concentrations declined from the proximal to distal colon. Acetate and propionate have roles in lipid and cholesterol synthesis as well as gluconeogenesis, whereas butyrate serves as the primary energy source for colonocytes. In addition, butyrate also has been shown to enhance colonic barrier defenses. Colonic mucosal scrapings obtained from colon cancer patients undergoing colectomy, followed by incubation with 0.1 mM of sodium butyrate, had increased ($p<0.001$; 80% more) mucin synthesis than controls incubated without sodium butyrate (Finnie et al., 1995). Paracellular transport in rat distal colonic epithelium also was altered upon exposure to 2 mmol/L of butyrate for 72 hr; transepithelial resistance was 83% higher ($p<0.05$) in butyrate-exposed epithelium compared to non-butyrate exposed controls (Mariadason et al., 1997).

Intestinal bacteria are a metabolic powerhouse, which upon stimulation can increase intestinal health. Fructan treatments have successfully captured the metabolic capabilities of intestinal bacteria and have shown extended benefits beyond providing vitamins, increased immunity against pathogens, and production of SCFA, but have displayed capabilities of increasing epithelial cell proliferation, reducing intestinal inflammation and restoring intestinal barrier function in obese models. Fructan prebiotics are capable of supporting a healthy intestinal microbial community, which has shown to benefit a low-grade inflammatory obese model.

Thesis objective

The general objective of this research was to identify mechanisms by which the integrity of the intestinal architecture and barrier are improved via supplementation of prebiotics with varying fermentation characteristics in an obese mouse model. Our main focus was on improvements of intestinal barrier function within this model. Therefore, we hypothesized that supplementation of prebiotics would lead to improved intestinal barrier function and increased expression of SCFA transporters and receptors, TJ proteins, AMP-kinase, and mucin (MUC2) genes. Additionally, we postulated that scFOS, a short-chain fructan prebiotic, would be rapidly fermented and have a greater response in the ileum and cecum of the mouse model, whereas inulin, a long-chain fructan prebiotic, would result in moderate improvements throughout the entire colon.

Literature Cited

Adams, R. B., Planchon, S. M., & Roche, J. K. (1993). IFN-γ modulation of epithelial barrier function. Time course, reversibility, and site of cytokine binding. *J .Immunol., 150*, 2356-2363.

Aliprantis, A. O., Yang, R. -B., Mark, M. R., Suggett, S., Devaux, B., Radolf, J. D., Klimpel G. R., Godowski, P., & Zychlinsky, A. (1999). Cell activation and apoptosis by bacterial lipoproteins through toll-like receptor-2. *Science, 285*, 736-739.

Ammori, B. F., Leeder, P. C., King, R. F., Barclay, G. R., Martin, I. G., Larvin, M., & McMahon, M. J. (1999). Early increase intestinal permeability in patients with severe acute pancreatitis: Correlation with endotoxemia, organ failure, and mortality. *J. Gastrointest. Surg., 3*, 252-262.

Aspenstrom-Fagerlund, B., Ring, L., Aspenstrom, P., Tallkvist, J., Ilback, N. -G., & Glynn, A. W. (2007). Oleic acid and docosahexaenoic acid cause an increase in the paracellular absorption of hydrophilic compounds in an experimental model of human absorptive enterocytes. *Toxicology, 237*, 12-23.

Atuma, C., Strugala, V., Allen, A., & Holm, L. (2001). The adherent gastrointestinal mucus gel layer: Thickness and physical state in vivo. *Am. J. Physiol. Gastrointest. Liver Physiol., 280*, G922-G929.

Awad, W. A., Ghareeb, K., & Bohm, J. (2010). Evaluation of the chicory inulin efficacy on ameliorating the intestinal morphology and modulating the intestinal electrophysiological properties in broiler chickens. *J. Anim. Physiol. Anim. Nutr., 95*, 65-72.

Backhed, F., Ding, H., Wang, T., Hooper, L. V., Koh, G. Y., Nagy, A., Semenkovich C. F., & Gordon, J. I. (2004). The gut microbiota as an environmental factor that regulates fat storage. *Proc. Natl. Acad. Sci.,101*, 15718-15723.

Barbier de La Serre, C., Ellis, C. L., Lee, J., Hartman, A. L., Rutledge, J. C., & Raybould, H. E. (2010). Propensity to high fat diet-induced obesity in rats is associated with changes in the gut microbiota and gut inflammation. *Am. J. Physiol. Gastrointest. Liver Physiol.,10*, G440-G448.

Benjamin, M. A., McKay, D. M., Yang, P. -C., Cameron, H., & Perdue, M. H. (2000). Glucagon-like peptide-2 enhances intestinal epithelial barrier function of both transcellular and paracellular pathways in the mouse. *Gut, 47*, 112-119.

Blay, G. L., Michel, C., Blottiere, H. M., & Cherbut, C. (1999). Prolonged intake of fructooligosaccharides induces a short-term elevation of lactic acid-producing bacteria and a persistent increase in cecal butyrate in rats. *J. Nutr., 129*, 2231-2235.

Bloom, S. M., Bijanki, V. N., Nava, G. M., Sun, L., Malvin, N. P., Donermeyer, D. L., Dunne, W. M. Jr., Allen, P. M., & Stappenbeck, T. S. (2011). Commensal bacteroides species induce colitis in host-genotype-specific fashion in a mouse model of inflammatory bowel disease. *Cell, 9*, 390-403.

Bouhnik, Y., Achour, L., Paineau, D., Riottot, M., Attar, A., & Bornet, F. (2007). Four-week short chain fructo-oligosaccharides ingestion leads to increasing fecal bifidobacteria and cholesterol excretion in healthy elderly volunteers. *Nutr. J., 6*, 42-49.

Bruewer, M., Luegering, A., Kucharzik, T., Parkos, C., Madara, J., Hopkins, A., & Nusrat, A. (2003). Proinflammatory cytokines disrupt epithelial barrier function by apoptosis-independent mechanisms. *J. Immunol., 171*, 6164-6172.

Brun, P., Castagliuolo, I., Di Leo, V., Buda, A., Pinzani, M., Palu, G., & Martines, D. (2007). Increased intestinal permeability in obese mice: New evidence in the pathogenesis of nonalcoholic steatohepatitis. *Am. J. Physiol. Gastrointest. Liver Physiol., 292,* G518-G525.

Cameron, H. L., & Perdue, M. H. (2005). Stress impairs murine intestinal barrier function: Improvement by glucagon-like peptide-2. *J. Pharmacol. Exp. Ther., 314*, 214-220.

Cani, P. D., Neyrinck, A. M., Faya, F., Knauf, C., Burcelin, R. G., Tuohy, K. M., Gibson, G. R., & Delzenne, N. M. (2007). Selective increase of bifidobacteria in gut microflora improve high-fat-diet-induced diabetes in mice through a mechanism associated with endotoxaemia. *Diabetologia, 50*, 2374-2383.

Cani, P. D., Possemiers, S., Van de Wiele, T., Guiot, Y., Everard, A., Rottier, O., Geurts, L., Naslain, D., Neyrinck, A., Lambert, D. M., Muccioli, G. G., & Delzenne, N. M. (2009). Changes in gut microbiota control inflammation in obese mice through a mechanism involving GLP-2-driven improvement of gut permeability. *Gut, 58*, 1091-1103.

Cani, P., Amar, J., Iglesias, M. A., Poggi, M., Knauf, C., Bastelica, D., Neyrinck, A. M., Fava, F., Tuohy, K. M., Chabo, C., Waget, A., Delmée, E., Cousin, B., Sulpice, T., Chamontin, B., Ferrières, J., Tanti, J. F., Gibson, G. R., Casteilla, L., Delzenne, N. M., Alessi, M. C., & Burcelin, R. (2007). Metabolic endotoxemia initiates obesity and insulin resistance. *Diabetes, 56*, 1761-1772.

Capaldo, C. T., & Nusrat, A. (2009). Cytokine regulation of tight junctions. *Biochem. Biophys. Acta., 1788*, 864-871.

Castellheim, A., Brekke, O. -L., Espevik, T., Harboe, M., & Mollnes, T. E. (2009). Innate immune responses to danger signals in systemic inflammatory response syndrome and sepsis. *J. Immunol., 69*, 479-491.

Corazziari, E. S. (2009). Intestinal mucus barrier in normal and inflamed colon. *J. Pediatr. Gastroenterol. Nutr., 48*, S54-S55.

Creely, S. J., McTernan, P. G., Kusminski, C. M., Fisher, F. M., Da Silva, N. F., Khanolkar, M., Evans, M., Harte, A. L., & Kumar, S. (2006). Lipopolysaccharide activates an innate immune system response in human adipose tissue in obesity and type 2 diabetes. *Am. J. Physiol. Endocrinol. Metab., 292*, E740-E747.

Erridge, C., Attina, T., Spickett, C. M., & Webb, D. J. (2007). A high-fat meal induces low-grade endotoxemia: Evidence of a novel mechanism of postprandial inflammation. *Am. J. Clin. Nutr., 86*, 1286-1292.

Fessler, M. B., Rudel, L. L., & Brown, J. M. (2009). Toll-like receptor signaling links dietary fatty acids to the metabolic syndrome. *Curr. Opin. Lipidol., 20*, 379-385.

Finnie, I. A., Dwarakanath, A. D., Taylor, B. A., & Rhodes, J. M. (1995). Colonic mucin synthesis is increased by sodium butyrate. *Gut, 36*, 93-99.

Frank, D. N., St. Amand, A. L., Feldman, R. A., Boedeker, E. C., Harpaz, N., & Pace, N. R. (2007). Molecular-phylogenetic characterization of microbial community imbalances in human inflammatory bowel diseases. *Proc. Natl. Acad. Sci., 104*, 13780-13785.

Furuse, M., Hata, M., Furuse, K., Yoshida, Y., Haratake, A., Suritani, Y., Noda, T., Kubo, A., & Tsukita, S. (2002). Claudin-based tight junctions are crucial for the mammalian epidermal barrier: A lesson from claudin-1 deficient mice. *J. Cell Biol., 156*, 1099 -1111.

Furuse, M., Itoh, M., Hirase, T., Nagafuchi, A., Yonemura, S., Tsukita, S., & Tsukita, S. (1994). Direct association of occludin with ZO-1 and its possible involvement in the localization of occludin at tight junction. *J. Cell Biol., 127*, 1617-1626.

Gardiner, K. R., Halliday, M. I., Barclay, G. R., Milne, L., Brown, D., Stephens, S., Maxwell R. J., & Rowlands, B. J. (1995). Significance of systemic endotoxemia in inflammatory bowel disease. *Gut, 36,* 897-901.

Gibson, G. R., & Roberfroid, M. B. (1995). Dietary modulation of the human colonic microbiota: Introducing the concept of prebiotics. *J. Nutr., 125,* 1401-1412.

Grizard, D., & Barthomeuf, C. (1999). Non-digestible oligosaccharides used as prebiotic agents: Mode of production and beneficial effects on animal and human health. *Reprod. Nutr. Dev., 39,* 563-588.

Groschwitz, K. R., & Hogan, S. P. (2009). Intestinal barrier function: Molecular regulation and disease pathogenesis. *J. Allergy Clin. Immunol., 124,* 3-14.

Gu, L., Li, N., Gong, J., Li, Q., Zhu, W., & Li, J. (2011). Berberine ameliorates intestinal epithelial tight-junction damage and down-regulates myosin light chain kinase pathways in a mouse model of endotoxinemia. *J. Infect. Dis., 203,* 1602-1612.

Guarner, F., & Malagelada, J. R. (2003). Gut flora in health and disease. *Lancet, 360,* 512-519.

Hamer, H. M., Jonkers, D., Venema, K., Vanhoutvin, S., Troost, F. J., & Brummer, R. J. (2008). Review article: The role of butyrate on colonic function. *Aliment. Pharmacol. Ther., 27,* 104-119.

Hang, C. H., Shi, J. X., Li, J. -S., Wu, W., & Yin, H. X. (2003). Alterations of intestinal mucosa structure and barrier function following traumatiac brain injury in rats. *World J. Gastroenterol., 9,* 2776-2781.

Hedemann, M. S., Theil, P. K., & Bach Knudsen, K. E. (2009). The thickness of the intestinal mucous layer in the colon of rats fed various sources of non-digestible carbohydrates is positively correlated with the pool of SCFA but negatively correlated with the proportion of butyric acid in digesta. *Brit. J. Nutr., 102,* 117-125.

Hernot, D. C., Boileau, T. W., Bauer, L. L., Middelbos, I. S., Murphy, M. R., Swanson, K. S. & Fahey, G.C. Jr. (2009). In vitro fermentation profiles, gas production rates, and microbiota modulation as affected by certain fructans, galactooligosaccharides, and polydextrose. *J. Agric. Food Chem., 57,* 1354-1361.

Hollander, D., Vadheim, C. M., Brettholz, E., Petersen, G. M., Delahunty, T., & Rotter, J. I. (1986). Increased intestinal permeability in patients with Crohn's disease and their relatives. A possible etiologic factor. *Ann. Intern. Med., 105,* 883-885.

Hotamisligil, G. S., Shargill, N. S., & Spiegelman, B. M. (1993). Adipose expression of tumor necrosis factor-alpha: Direct role in obesity-linked insulin resistance. *Science, 259,* 87-91.

Huber, W., Herrmann, G., Schuster, T., Phillip, V., Saugel, B., Schultheiss, C., Hoellthaler, J., Gaa, J., Hartel, M., Schmid, R. M., & Reindl, W. (2010). Life-threatening complications of Crohn's disease and ulcerative colitis: A systematic analysis of admissions to an ICU during 18 years. *Dtsch. Med. Wochenschr., 135,* 668-674.

Inan, M. S., Rasoulpour, R. J., Yin, L., Hubbard, A. K., Rosenberg, D. W., & Giardina, C. (2000). The luminal short-chain fatty acid butyrate modulates NF-κB activity in a human colonic epithelial cell line. *Gastroenterol., 118,* 724-734.

Inokuchi, S., Tsukamoto, H., Park, E., Liu, Z. X., Brenner, D. A., & Seki, E. (2011). Toll-like receptor 4 mediates alcohol-induced steatohepatitis through bone marrow-derived and endogenous live cells in mice. *Alcohol Clin. Exp. Res., 35,* 1-10.

Itoh, M., Furuse, M., Morita, K., Kubota, K., Saitou, M., & Tsukita, S. (1999). Direct binding of three tight junction-associated MAGUK's, ZO-1, ZO-2 and ZO-3, with the COOH termini of claudins. *J. Cell Biol., 147*, 1351-1363.

John, L. J., Fromm, M., & Schulzke, J. D. (2011). Epithelial barriers in intestinal inflammation. *Antioxid. Redox Signal, 15*, 1-16.

Katsuno, T., Umeda, K., Matsui, T., Hata, M., Tamura, A., Itoh, M., Takeuchi, K., Fujimori, T., Nabeshima, Y., Noda, T., Tsukita, S., & Tsukita, S. (2008). Deficiency of zonula occludens-1 causes embryonic lethal phenotype associated with defected yolk sac angiogenesis and apoptosis of embryonic cells. *Mol. Biol. Cell., 19*, 2465-2475.

Kelly, G. (2008). Inulin-type prebiotics - A review: Part 1. *Altern. Med. Rev., 13*, 315-329.

Khoo, J. J., Forster, S., & Mansell, A. (2011). Toll-like receptors as interferon-regulated genes and their role in disease. *J. Interferon Cytokine Res., 31*, 13-25.

Kien, C. L., Blauwiekel, R., Bunn, J. Y., Jetton, T. L., Frankel, W. L., & Holst, J. J. (2007). Cecal infusions of butyrate increases intestinal cell proliferation in piglets. *J. Nutr., 137*, 916-922.

Kleessen, B., Hartmann, L., & Blaut, M. (2003). Fructans in the diet cause alterations of intestinal mucosal architecture, released mucins and mucosa-associated bifidobacteria in gnotobiotic rats. *Brit. J. Nutr., 89*, 597-606.

Kotlowski, R., Bernstein, C. N., Sepehri, S., & Krause, D. O. (2007). High prevalence of *Escherichia coli* belonging to the B2+D phylogenetic group in inflammatory bowel disease. *Gut, 56*, 669-675.

Krzystek-Korpacka, M., Mierzchala, M., Neubauer, K., Durek, G., & Gamian, A. (2011). Midkine, a multifunctional cytokine, in patients with severe sepsis and septic shock: A pilot study. *Shock , 35*, 471-477.

Laugerette, F., Vors, C., Peretti, N., & Michalski, M. C. (2010). Complex links between dietary lipids, endogenous endotoxins and metabolic inflammation. *Biochimie, 93*, 39-45.

Laukoetter, M., Nava, P., Lee, W., Severson, E., Capaldo, C., Babbin, B., Williams, I. R., Koval, M., Peatman, E., Campbell, J. A., Dermody, T. S., Nusrat, A., & Parkos, C. A. (2007). JAM-A regulates permeability and inflammation in the intestine in vivo. *J. Exp. Med., 204*, 3067-3076.

Ley, R. E., Bäckhed, F., Turnbaugh, P., Lozupone, C. A., Knight, R. D., & Gordon, J. I. (2005). Obesity alters gut microbial ecology. *Proc. Natl. Acad. Sci., 102*, 11070-11075.

Ley, R., Turnbaugh, P., Klein, S., & Gordon, J. (2006). Human gut microbes associated with obesity. *Nature, 444*, 1022-1023.

Liu, C., Li, A., Weng, Y. B., Duan, M. L., Wang, B. E., & Zhang, S. W. (2009). Changes in intestinal mucosal immune barrier in rats with endotoxemia. *World J. Gastroenterol., 15*, 5843-5850.

Ma, T. Y., Iwamoto, G. K., Hoa, N. T., Akotia, V., Pedram, A., Boivin, M. A., & Said, H. M. (2004). TNF-alpha induced increase in intestinal epithelial tight junction permeability requires NF-κB activation. *Am. J. Physiol. Gastrointest. Liver Physiol., 286*, G367-G376.

Mariadason, J. M., Barkla, D. H., & Gibson, P. R. (1997). Effect of short-chain fatty acids on paracellular permeability in Caco-2 intestinal epithelium model. *Am. J. Physiol.,* 272: G705-G712.

Maury, E., & Brichard, S. (2010). Adipokine dysregulation, adipose tissue inflammation and metabolic syndrome. *Mol. Cell. Endocrinol., 314*, 1-16.

Mitic, L., Van Itallie, M. C., & Anderson, M. J. (2000). Molecular physiology and pathophysiology of tight junctions I. Tight junction structure and function: Lessons from mutant animals and proteins. *Am. J. Physiol. Gastrointest. Liver Physiol., 279*, G250-G254.

Mitsuoka, T. (1990). Bifidobacteria and their role in human health. *J. Ind. Microbiol., 6*, 263-268.

Mohamed-Ali, V., Goodrick, S., Rawesh, A., Katz, D. R., Miles, J. M., Yudkin, J. S., Klein, S., & Coppack, S. W. (1997). Subcutaneous adipose tissue releases interleukin-6, but not tumor necrosis factor-alpha, in vivo. *J. Clin. Endocrinol. Metab., 82*, 4196-4200.

Nanji, A., Khettry, U., & Sadrzadeh, S. (1994). *Lactobacillus* feeding reduces endotoxemia and severity of experimental alcoholic liver (disease). *Exp. Biol. Med., 205*, 243-247.

Neurath, M. F., Becker, C., & Barbulescu, K. (1998). Role of NF-κB in immune and inflammatory responses in the gut. *Gut, 43*, 856-860.

Park, E., Thomson, A., & Clandinin, M. (2010). Protection of intestinal occludin tight junction protein by dietary gangliosides in lipopolysaccharide-induced acute inflammation. *J. Pediatr. Gastroenterol. Nutr., 50*, 321-328.

Pasternak, B. A., D'Mello, S., Jurickova, I. I., Han, X., Wilson, T., Flick, L., Petiniot, L., Uozumi, N., Divanovic, S., Traurnicht, A., Bonkowski, E., Kugathasan, S., Karp, C. L., & Denson, L. A. (2010). Lipopolysaccharide exposure is linked to activation of the acute phase response and growth failure in pediatric Crohn's disease and murine colitis. *Inflamm. Bowel Dis., 16*, 856-869.

Peng, L., Li, Z. -R., Green, R. S., Holzman, I. R., & Lin, J. (2009). Butyrate enhance the intestinal barrier by facilitating tight junction assembly via activation of AMP-activated protein kinase in Caco-2 cell monolayers. *J. Nutr., 139*, 1619-1625.

Raetz, C. R., & Whitfield, C. (2002). Lipopolysaccharide endotoxins. *Annu. Rev.Biochem.*, 71, 635-700.

Reikvam, D. H., Erofeev, A., Sandvik, A., Grcic, V., Lars Jahnsen, F., Gaustad, P., McCoy, K. D., Macpherson, A. J., Meza-Zepeda, L. A., & Johansen, F. E. (2011). Depletion of murine intestinal microbiota: Effects on gut mucosa and epithelial gene expression. *Plos One, 6*, e17996. doi:10.1371/journal.pone.0017996.

Rescigno, M. (2011). The intestinal epithelial barrier in the control of homeostasis and immunity. *Cell, 32*, 256-265.

Roberfroid, M. B., Van Loo, J. A., & Gibson, G. R. (1998). The bifidogenic nature of chicory inulin and its hydrolysis products. *J. Nutr., 128*, 11-19.

Roberfroid, M., Gibson, G. R., Hoyles, L., McCartney, A. L., Rastall, R., Rowland, I, Wolvers, D., Watzl, B., Szajewska, H., Stahl, B., Guarner, F., Respondek, F., Whelan, K., Coxam, V., Davicco, M. J., Léotoing, L., Wittrant, Y., Delzenne, N. M., Cani, P. D., Neyrinck, A. M., & Meheust, A. (2010). Prebiotic effects: Metabolic and health benefits. *Brit. J. Nutr., 104*, S3-S51.

Rockett, B. D., Salameh, M., Carraway, K., Morrison, K., & Shaikh, S. R. (2010). n-3 PUFA improves fatty acid composition, prevents palmitate-induced apoptosis, and differentially modifies B cell cytokine secretion in vitro and ex vivo. *J. Lipid Res., 51*, 1284-1296.

Russo, G. L. (2009). Dietary n-6 and n-3 polyunsaturated fatty acids: From biochemistry to clinical implications in cardiovascular prevention. *Biochem. Pharmacol., 77*, 937-946.

Schulzke, J., Ploeger, S., Amasheh, M., Fromm, A., Zeissig, S., Troeger, H., Richter, J., Bojarski, C., Schumann, M., & Fromm, M. (2009). Epithelial tight junction in intestinal inflammation. *Ann. N.Y. Acad. Sci., 1165,* 294-300.

Shen, L., Black, E. D., Witkowski, E. D., Lencer, W. I., Guerriero, V., Shneeberger, E. E., & Turner, J. R. (2006). Myosin light chain phosphorylation regulates barrier function by remodeling tight junction structure. *J. Cell Sci., 119,* 2095-2106.

Shi, H., Kokoeva, M. V., Inouye, K., Tzameli, I., Yin, H., & Flier, J. S. (2006). TLR4 links innate immunity and fatty acid-induced insulin resistance. *J. Clin. Invest., 116,* 3015-3025.

Shimizu, M. (2010). Interaction between food substances and the intestinal epithelium. *Biosci. Biotechnol. Biochem.,74,* 232-241.

Simopoulos, A. (2006). Evolutionary aspects of diet, the omega-6/omega-3 ratio and genetic variation: Nutritional implications for chronic diseases. *Biomed. Pharmacother., 60,* 502-507.

Simopoulos, A. (2002). The importance of the ratio of omega-6/omega-3 essential fatty acids. *Biomed. Pharmacother.,56,* 365-379.

Smith, K., McCoy, K. D., & Macpherson, A. J. (2007). Use of axenic animals in studying the adaptation of mammals to their commensal intestinal microbiota. *Immunol., 19,* 59-69.

Song, H. L., Lv, S., & Liu, P. (2009). The roles of tumor necrosis factor-alpha in colon tight junction protein expression and intestinal mucosa structure in a mouse model of acute liver failure. *BMC Gastroenterol., 9,* 1-9.

Suzuki, T., & Hara, H. (2010). Dietary fat and bile juice, but not obesity, are responsible for the increase in small intestinal permeability induced through the suppression of tight junction protein expression in LETO and OLETF rats. *Nutr. Metab., 7,* 7-19.

Suganami, T., Tanimoto-Koyama, K., Nishida, J., Itoh, M., Yuan, X., Mizuarai, S., Kotani, H., Yamaoka, S., Miyake, K., Aoe, S., Kamei, Y., & Ogawa, Y. (2007). Role of the toll-like receptor 4/NF-κB pathway in saturated fatty acid-induced inflammatory changes in the interaction between adipocytes and macrophages. *Arterioscler. Thromb. Vasc. Biol., 27,* 84-91.

Taniguchi, Y., Yoshioka, N., Nakata, K., Nishizawa, T., Inagawa, H., Kohchi, C., & Soma, G. (2009). Mechanism for maintaining homeostasis in the immune system of the intestine. *Anticancer Res., 29,* 4855-4860.

Trayhurn, P., Wang, B., & Wood, I. S. (2008). Hypoxia in adipose tissue: A basis for the dysregulation of tissue function in obesity? *Brit. J. Nutr., 100,* 227-235.

Usami, M., Muraki, K., Iwamoto, M., Ohata, A., Matsushita, E., & Miki, A. (2001). Effect of eicosapentaenoic acid (EPA) on tight junction permeability in intestinal monolayer cells. *J. Clin. Nutr., 20,* 351-359.

Van Itallie, C. M., & Anderson, J. M. (2006). Claudins and epithelial paracellular transport. *Ann. Rev. Physiol., 68,* 403-429.

Velasco, N. (2006). Gut barrier in the critically ill patient: Facts and trends. *Rev. Med. Chile., 134,* 1033-1039.

Virtue, S., & Vidal-Puig, A. (2010). Adipose tissue expandability, lipotoxicity and the metabolic syndrome - An allostatic perspective. *Biochem. Biophys. Acta, 1801,* 338-349.

Vital signs: State-specific obesity prevalence among adults---United states, 2009. (2010, August 3). Retrieved December 30, 2011, from CDC: Centers for Disease Control and Prevention: http://www.cdc.gov.

Weisberg, S. P., McCann, D., Desai, M., Rosenbaum, M., Leibel, R., & Ferrante, Jr., A. W. (2003). Obesity is associated with macrophage accumulation in adipose tissue. *J. Clin. Invest., 112,* 1796-1808.

Xiao, F., Juric, M., Li, J., Riederer, B., Yeruva, S., Singh, A. K., Zheng, L., Glage, S., Kollias, G., Dudeja, P., Tian, D. A., Xu, G., Zhu, J., Bachmann, O., & Seidler, U. (2011). Loss of downregulation in adenoma (DRA) impairs mucosal HCO_3^- secretion in murine ileocolonic inflammation. *Inflamm. Bowel Dis., 18, 101-111.*

Xu, J., Kausalya, J., Phua, D. C., Ali, S. M., Hossain, Z., & Hunziker, W. (2008). Early embryonic lethality of mice lacking ZO-2, but not ZO-3, reveals critical and nonredundant roles for individual zonula occludens proteins in mammalian development. *Mol. Cell. Biol., 28,* 1669-1678.

Ye, J., Gao, Z., Yin, J., & He, Q. (2007). Hypoxia's a potential risk factor for chronic inflammation and adiponectin reduction in adipose tissue of ob/ob and dietary obese mice. *Am. J. Physiol. Endocrinol. Metab., 293,* E1118-E1128.

Youakim, A., & Ahdieh, M. (1999). Interferon-γ decreases barrier function in T84 cells by reducing ZO-1 levels and disrupting apical actin. *Am. J. Physiol. Gastro. Liver Physiol., 276,* G1279-G1288.

Yu, D., Marchiando, A. M., Weber, C. R., Raleigh, D. R., Wang, Y., Shen, L., & Turner, J. R. (2010). MLCK-dependent exchange and actin binding region-dependent anchoring of ZO-1 regulate tight junction barrier function. *Proc. Natl. Acad. Sci., 107,* 8237-8241.

Zeissig, S., Burgel, N., Gunzel, D., Richter, J., Mankertz, J., Wahnschaffe, U., Kroesen, A. J., Zeitz, M., Fromm, M., & Schulzke, J. D. (2007). Changes in expression and distribution of claudin 2, 5 and 8 lead to discontinuous tight junctions and barrier dysfunction in active Crohn's disease. *Gut, 56,* 61-72.

Zhang, H., DiBaise, J. K., Zuccolo, A., Kudrna, D., Braidotti, M., Yu, Y., Parameswaran, P., Crowell, M. D., Wing, R., Rittmann, B. E. & Krajmalnik-Brown, R. (2009). Human gut microbiota in obesity and after gastric bypass. *Proc. Natl. Acad. Sci., 106,* 2365-2370.

Zhang, J., Du, X., Zhang, H., Li, M., Xiao, G., Wu, J., & Gan, H. (2010). Breakdown of the gut barrier in patients with mutiple organ dysfunction syndrome is attenuated by continuous blood purification: Effects on tight junction structural proteins. *Int. J. Artif. Organs, 33,* 5-14.

Zhang, J., Yuan, C., Hua, G., Tong, R., Luo, X., & Ying, Z. (2010). Early gut barrier dysfunction in patients with severe acute panceatitis: Attenuated by continuous blood purification treatment. *Int. J. Artif. Organs, 33,* 706-715.

Zhao, H., Lu, Z., Bie, X., & Lu, F. (2005). Analysis of positional distribution of fatty acids in triacylglycerols from lard by high performance liquid chromatography. *Se Pu, 23,* 142-145.

Zhong, W., McClain, C. J., Cave, M., Kang, Y. J., & Zhou, Z. (2010). The role of zinc deficiency in alcohol-induced intestinal barrier dysfunction. *Am. J. Physiol. Gastrointest. Liver Physiol., 298,* G625-G633.

Zhu, B., Wang, X., & Li, L. (2010). Human gut microbiome: the second genome of human body. *Protein Cell, 1,* 718-725.

Chapter 3

Effects of fructan source and degree of polymerization on intestinal barrier function and histomorphology characteristics in obese C57BL/6 mice

Abstract

Obesity is linked to increased intestinal permeability that may contribute to low grade inflammation. Fructan prebiotics have been demonstrated to increase intestinal resistance and decrease systemic inflammation. The objective of this study was to test the effects of prebiotics on intestinal permeability, morphology, and gene expression in an obese mouse model. Obese, 18-wk old, C57BL/6 mice were randomized to high-fat (45% of kcal) diets containing 5% cellulose, 10% cellulose, 10% short-chain fructooligosaccharides (scFOS) or 10% inulin and fed for 28 d. Distal ileum, cecum, and colon samples were collected for Ussing chamber, histomorphology, and qRT-PCR analyses. The effects of treatment were tested using the Mixed Models procedure of SAS. Among treatments, mice fed scFOS and inulin had greater ($p<0.05$) intestinal transmural resistance compared to mice fed 5% cellulose. MCT-1 expression was greater ($p<0.05$) in the distal colon of mice fed 10% cellulose compared to 10% inulin. ZO-1 expression was lower ($p<0.05$) in mice fed inulin compared to other treatments. Occludin mRNA abundance was lowest ($p<0.05$) in fructan sources compared to cellulose. When comparing 5% vs. 10% cellulose treatments using contrasts, 10% cellulose led to greater ($p<0.05$) intestinal crypt depth in all intestinal regions, except the distal colon. Mice fed 5% vs. 10% cellulose, however, had greater ($p<0.05$) ileal villus height: crypt depth ratio, ileal MUC2 mRNA abundance, proximal colon AMPK mRNA abundance, and occludin mRNA abundance in the proximal and distal colon regions. When comparing fructan vs. cellulose treatments using contrasts, fructans resulted in a greater ($p<0.05$) transmural resistance and crypt depth when all intestinal regions were combined. In contrast, fructan-fed mice had lower ($p<0.05$) mRNA

abundance of ZO-1 and occludin when all intestinal regions were combined (Table 3.5). Fructan consumption resulted in lower ($p<0.05$) ileal MUC2 and occludin mRNA abundance, cecal occludin mRNA abundance, proximal colon MCT-1, ZO-1, AMPK, and occludin mRNA abundance, and distal colon ZO-1, AMPK, and occludin mRNA abundance. Cecal AMPK mRNA abundance was greater ($p<0.05$) in fructan-fed compared to cellulose-fed mice. Pearson coefficient correlations indicated correlations between MCT-1 and distal colon ZO-1 ($r = 0.77$, $p<0.05$) and occludin mRNA abundance ($r = 0.66$, $p<0.05$). AMPK correlated with ZO-1 mRNA abundance ($r = > 0.60$, $p<0.05$) in all regions of the intestinal tissue of C57BL/6 mice. Lastly, ZO-1 mRNA abundance correlated with distal colon epithelial resistance ($r = 0.51$, $p<0.05$). Collectively, these data may suggest mechanisms by which equivalent quantities of fructan prebiotics and non-fermentable fibers affect intestinal barrier function.

Introduction

The intestinal barrier is essential in protecting the host from ingested pathogens and toxins and commensal intestinal bacteria. The main cause of increased intestinal permeability has been found to be overt inflammation, which is observed in disorders such as ulcerative colitis and Crohn's disease, potentially causing sepsis (Hollander et al., 1986; Gardiner et al., 1995; Laukoetter et al., 2008; Huber et al., 2010). Intestinal barrier function is not only important in maintaining gastrointestinal health, but also appears to apply to obesity because of recent findings of increased intestinal permeability in obese mice. Brun et al. (2006) reported decreased ($p<0.05$; 55% lower) intestinal epithelial resistance in *ob/ob* mice than wild-type controls. That study also reported reduced occludin and ZO-1 tight junction protein abundance in the ileum. Barbier de La Serre et al. (2010) also reported increased intestinal permeability and decreased occludin at the tight junction in diet-induced obesity-prone rats. This evidence is alarming, yet few interventions have been reported effective in treating this decline in gut health.

Prebiotics may have positive effects in decreasing intestinal permeability, yet there is little evidence showing associations between prebiotics and intestinal barrier function in an obese model. Cani et al. (2009) showed that supplementation of oligofructose, a fructan prebiotic, increased intestinal resistance and ZO-1 protein abundance in obese C57BL/6 mice fed a high-fat (70% of kcal) diet. Given the extreme diets fed in that study, however, further research is required using more realistic diets and to identify potential mechanisms by which prebiotics may be improving barrier function. Therefore, with this evidence in mind, the primary objective of this study was to evaluate the effects of fructan prebiotics of different degree of polymerization (DP) on intestinal barrier function in an obese mouse model.

Materials and Methods

All animal care procedures were approved by the University of Illinois Institutional Animal Care and Use Committee prior to animal experimentation.

Animals and diets

Twenty-four 18-wk old C57BL/6 mice (Jackson Laboratory, Bar Harbor, ME) were used in a completely randomized design. Mice were assigned a pelleted American Institute of Nutrition-1993 growth (AIN-93G)-based diet containing 45% kcal from fat and 5% cellulose during a 2-wk acclimation period **(Table 3.1 and Table 3.2)**. Mice then were randomized to four pelleted AIN-93G-based diets containing 45% kcal from fat containing either non-fermentable dietary fiber or fructan-derived prebiotics. Dietary treatments included: 1) 5% cellulose; 2) 10% cellulose; 3) 10% short-chain fructooligosaccharides (scFOS); and 4) 10% inulin, and were fed *ad libitum* for 4 wk. The mice were individually housed in shoe-box cages in the Institute for Genomic Biology Animal Facility at the University of Illinois. Environmental conditions were controlled with a 12-h light-dark cycle with *ad libitum* feeding, free access to water, weekly

health inspections, and body weight measurements. Visible offered, but refused treatments were recorded daily.

Blood and tissue collection

Upon completion of the 4-wk intervention, mice were fasted for 6 h, followed by CO_2 asphyxiation. Blood was collected via cardiac puncture. Intestinal sections were collected from the ileum, cecum, proximal colon, and distal colon for intestinal morphology, quantitative reverse transcriptase-polymerase chain reaction (qRT-PCR), and intestinal permeability measurements. All intestinal sections were rinsed in modified Kreb's buffer solution and placed in formalin for histomorphological analysis or modified Kreb's buffer solution for electrophysical analysis of intestinal resistance. A third portion of each tissue was flash frozen in liquid nitrogen and stored at -80°C until further analysis.

Intestinal permeability measurement using modified Ussing chambers

Intestinal samples were resected, cut longitudinally, and mounted into modified Ussing chambers (Physiological Instruments, Inc., San Diego, CA) exposing 0.031 cm^2 of the mucosal and serosal sides to 8 mL of oxygenated (95% O_2 and 5% CO_2) modified Krebs buffer solution maintained at 37°C by use of a circulation water bath (IsoTemp 2006S, Fisher Scientific, Itasca, IL). After allowing 10-20 min to reach equilibrium, transmural resistance (Ohm x cm^2) was measured. The modified Ussing chambers were connected to dual channel voltage/current clamps (VCC MC2, Physiological Instruments) with a computer interface that allowed for real time data acquisition and analysis with Acquire and Analyze software (Physiological Instruments).

Intestinal histomorphology measurement

Intestinal samples were fixed in formalin and embedded in paraffin and sectioned to 4 μm thickness using a microtome and stained with hematoxylin and eosin at the University of Illinois at Urbana-Champaign Veterinary Pathology Laboratory. Ileal villus height, ileal crypt depth, cecal crypt depth, and colon crypt depth measurements were performed on 15 well-oriented, intact villi and crypts using Axiovision AC software and an AxioCam MRc5 (Carl Zeiss, Obercochen, Germany).

RNA extraction and analyses

Total cellular RNA was isolated from tissue samples using the RNeasy Kit (Qiagen, Valencia, CA). RNA concentration was determined using a ND-1000 spectrophotometer (Nanodrop Technologies, Wilmington, DE). RNA integrity was confirmed by gel electrophoresis prior to qRT-PCR analyses. TaqMan Gene Expression Assays primer-probe sets (Applied Biosystems, Foster City, CA) were used for each gene of interest [monocarboxylic transporter-1 (MCT-1), monocarboxylic transporter-4 (MCT-4), solute carrier family 5, member 8 (SLC5A8), solute carrier family 5, member 12 (SLC5A12), G-protein coupled receptor-43 (GPR43), AMP-kinase (AMPK), mucin 2 (MUC2), zonula occluden-1 (ZO-1), occludin, and taste receptor type 2-38 (T2R38, bitter taste receptor)]. Real-time two-step RT-PCR was performed using the Applied Biosystems 7900HT Real-Time PCR System (Applied Biosystems). Each gene was tested in triplicate, using eukaryotic 18S rRNA as a control in parallel with genes of interest. Data were normalized to 18S rRNA and expressed as a ratio to the 18S rRNA signal.

Chemical analyses

Diet samples were analyzed for dry matter and organic matter according to AOAC (1984). Crude protein was determined using a Leco Nitrogen/Protein Determinator (model FP-2000, Leco Corporation, St. Joseph, MI) (AOAC, 1995). Fat concentrations were measured by acid hydrolysis (AACC, 1983) followed by ether extraction (Budde, 1952). Gross energy was measured by the use of a bomb calorimeter (Model 1261, Parr Instruments, Moline, IL). Total dietary fiber (TDF) concentrations were determined using methods described by Prosky et al. (1985). Calculated TDF was based on purities provided by Orafti (Tienen, Belgium) for inulin (Raftiline HP; 95.5%), Research Diets (New Brunswick, NJ) for cellulose (Solka-Floc; 99%), and GTC Nutrition (Golden, CO) for scFOS (NutraFlora; 95%).

Statistical analyses

Histomorphology, transmural resistance, and PCR data were analyzed using the Mixed Models procedure of SAS ® (SAS Institue, Cary, NC). Data were transformed to obtain normality (using the log and square root transformations, respectively). Statistical analysis and differences were determined utilizing the transformed data; however, observed means are presented in the tables, figures, and text. The fixed effect of diet across all regions, and within each region was tested. Sampling day was considered a random effect. Differences were determined using a Fisher-protected LSD with a Tukey adjustment to control for experiment-wise error. A probability of $P \leq 0.05$ was accepted as statistically significant. Intestinal morphology, intestinal resistance, and gene expression data sets were analyzed for Pearson correlation coefficients by using the PROC CORR procedure of SAS® (SAS Institue, Cary, NC). A probability of $P \leq 0.05$ was accepted as statistically significant.

Results

Mean daily food intake and body weight

Mean daily food intake (g/d) during the 4-wk treatment period was greater ($p<0.05$) in mice fed 10% cellulose compared to those fed 5% cellulose, 10% scFOS or 10% inulin (**Figure 3.1**).

Body weights at baseline (39.5 ± 0.9, 39.4 ± 0.9, 38.9 ± 0.9, and 37.8 g ± 0.9 for 5% cellulose, 10% cellulose, 10% scFOS, and 10% inulin, respectively) were lower ($P<0.0001$) than those after 4 wk (42.0 ± 0.5, 43.6 ± 0.5, 42.1 ± 0.5, and 41.9 g ± 0.5 for 5% cellulose, 10% cellulose, 10% scFOS, and 10% inulin, respectively) for all treatments (**Figure 3.2**). 10% cellulose-fed mice were heavier ($p<0.01$) at 24 wk compared to remaining treatments.

Histomorphology

Intestinal histomorphological effects of prebiotic supplementation were assessed by measuring ileal villus height and crypt depth and crypt depth of the cecum, proximal colon, and distal colon (**Table 3.3 and Figure 3.3**). Mice fed scFOS had substantial improvements in intestinal architecture. Specifically, ileal villus height was greater ($p<0.05$) in mice fed scFOS compared to those fed 5% cellulose and ileal and cecal crypt depth was greater ($p<0.05$) in mice fed scFOS or inulin compared to those fed 5% and 10% cellulose. Inulin-fed mice had greater ($p<0.05$) proximal colon crypt depth compared to 10% scFOS- and 10% cellulose-fed mice. Lastly, mice fed 10% cellulose had increased ($p<0.05$) distal colon crypt depth compared to mice fed 10% scFOS. The villus height:crypt depth ratio was greater ($p<0.05$) in mice fed 5 or 10% cellulose compared to mice fed scFOS or inulin.

Intestinal transmural resistance

Intestinal transmural resistance of the ileum, cecum, proximal colon, and distal colon of C57BL/6 mice was evaluated by assessing the resistance in a Ussing chamber (**Figures 3.4 and 3.5**). The main effect of diet among regions was not significant, however, mice supplemented with inulin and scFOS had greater ($p<0.05$) intestinal transmural resistance in the cecum and distal colon, respectively, compared to cellulose-fed mice.

SCFA transporter and receptor mRNA abundance

SCFA transporter and receptor mRNA abundance was assessed to determine the possible involvement of these genes in connection with intestinal permeability (**Figure 3.6 – Figure 3.11**). The main effect of diet on SCFA transporters and receptor were not significant; however, MCT-1 mRNA abundance increased ($p<0.05$) in the distal colon of mice-fed 10% cellulose compared to inulin-fed mice. Yet, MCT-4 and GPR43 mRNA abundance was not significant in any region of murine intestine.

MUC2 mRNA abundance

In order to determine the involvement of other factors contributing to intestinal resistance, expression of MUC2 was assessed using qPCR (**Figure 3.12 & Figure 3.13**). A significant increase ($p<0.05$) of MUC2 mRNA abundance was observed in the ileum of mice fed 10% cellulose compared to fructan-treated mice. However, the main effect of diet among regions was not significant.

AMPK, ZO-1, and occludin mRNA abundance

New evidence by Peng et al. (2009) demonstrated a connection between AMPK, which is an energy sensor of cellular activity (i.e. assesses the presence of ATP) and the tight junction proteins, ZO-1 and occludin. The main effect of diet on AMPK mRNA abundance was not

significant among treatments (**Figure 3.14 – Figure 3.19**). However, specific to the cecum, 10% scFOS-fed mice produced greater ($p<0.05$) AMPK mRNA abundance vs. 5% cellulose-fed mice. Inulin-fed mice had substantially lower ($p<0.05$) AMPK mRNA abundance in the distal colon compared to cellulose and scFOS-fed mice. Across all regions, ZO-1 mRNA abundance was significantly lower ($p<0.05$) in inulin-fed mice compared to cellulose and scFOS treatments. Inulin-fed mice also had lower ($p<0.05$) ZO-1 mRNA abundance in the distal colon versus cellulose and scFOS-fed mice. Among all regions, cellulose-fed mice had greater ($p<0.05$) occludin mRNA abundance than fructan-fed mice. Ileal, proximal colon, and distal colon occludin mRNA abundance was also lower ($p<0.05$) in inulin-fed mice compared to cellulose- and scFOS-fed mice. Cecal occludin, however, was lower ($p<0.05$) in 10% cellulose- and 10% scFOS-fed mice compared to those fed 5% cellulose.

Contrasts of 5% cellulose vs. 10% cellulose treatments and cellulose vs. fructan treatments

Contrast statements were used to determine any differences in resistance, mRNA abundance, and histomorphology characteristics between mice fed 5% cellulose and 10% cellulose (**Table 3.4**). Overall, 10% cellulose was found to increase ($p<0.05$) intestinal crypt depth in all regions, except the distal colon. Mice fed 5% cellulose, however, had greater ($p<0.05$) ileal villus height: crypt depth ratio, ileal MUC2 mRNA abundance, proximal colon AMPK mRNA abundance, and occludin mRNA abundance in the proximal and distal colon regions.

Contrast statements also were used to determine differences in mice fed fructans compared to those fed cellulose. Fructan consumption led to greater ($p<0.05$) transmural resistance and crypt depth when all intestinal regions were combined. In contrast, fructan-fed mice had lower ($p<0.05$) mRNA abundance of ZO-1 and occludin when all intestinal regions

were combined (**Table 3.5**). Fructan consumption resulted in lower ($p<0.05$) ileal MUC2 and occludin mRNA abundance, cecal occludin mRNA abundance, proximal colon MCT-1, ZO-1, AMPK, and occludin mRNA abundance, and distal colon ZO-1, AMPK, and occludin mRNA abundance. Cecal AMPK mRNA abundance was greater ($p<0.05$) in fructan-fed compared to cellulose-fed mice.

Correlations between intestinal histomorphology, transmural resistance, and mRNA abundance

Many significant correlations ($p<0.05$) were observed between intestinal histomorphology, transmural resistance, and gene expression (**Tables 3.6 and 3.7**). Ileal MUC2 expression was negatively correlated with ileal villus height, but positively correlated with ileal transmural resistance. Proximal colon AMPK expression was positively correlated with proximal colon crypt depth, while distal colon ZO-1 expression was positively correlated with distal colon transmural resistance. AMPK expression was positively correlated with the expression of MCT-1 (distal colon), MCT-4 (distal colon), ZO-1 (all regions), and occludin (distal colon). MCT-1 expression was positively correlated with the expression of ZO-1 (ileum, cecum, and distal colon) and occludin (distal colon), while MCT-4 expression was positively correlated with the expression of ZO-1 (cecum and distal colon). Finally, occludin expression was positively correlated with ZO-1 expression (proximal and distal colon).

Discussion

The current study was pursued to understand the risk of obesity and associated comorbidites, such as low-grade inflammation, on increased intestinal barrier permeability. Over 70% of Americans are overweight or obese due to poor dietary habits. Evidence is limited in showing low-grade inflammation and intestinal barrier permeability in human subjects, however, a pilot study performed by Brignardello et al. (2010) showed obese subjects (BMI 35.9, n=13)

had significantly higher C-reactive protein serum levels compared to normal weight controls (BMI 23.5, n=11). In addition, the obese group had higher gut permeability of mannitol (151 mg) compared to that of normal weight individuals (115 mg). These data were not significant, but showed the presence of intestinal barrier permeability within this small group of subjects and suggested a need for an intervention.

Our study utilized C57BL/6 mice fed high-fat diets to simulate the obesogenic states of Americans. Furthermore, this model also presents with diabetes mellitus and cardiovascular disease, which are common co-morbidities associated with obesity; our model presented with low-grade inflammation (data not shown) and increased body weight upon high dietary fat intake, which epitomizes Western behavior and diet. Our study did not utilize control mice, however, normal growth data reported from Jackson Laboratory (Jackson Laboratory, Bar Harbor, ME) on the weight gain of C57BL/6 mice fed a 6% fat diet showed a steady incline in the weight (13.59 g at 4 wk to 29.97 g at 16 wk of age) at which the weight did not plateau. Therefore we were confident a low-fat diet (control group fed a lower fat diet) would produce a phenotype lower in weight than our mice fed a 45% fat diet.

In humans, the bacterial count per gram wet weight of contents is greatest in the proximal colon due to high substrate availability, enabling the growth of diverse bacteria (Leser & Molbak, 2009). Intestinal microbiota possess many fermentative enzymes not possessed by the host, and are capable of enzymatically breaking down ingested fermentable products and releasing substrates, such as short-chain fatty acids (SCFA), methane, phenols and lactate (Leser & Molbak, 2009; Roberfroid et al., 2010). Substrate availability continues to be high at cecal entry, and will undergo fermentation yielding approximately 75% more SCFA than distal colon fermentation (Macfarlane & Macfarlane, 2003). The fermentative capabilities of intestinal

bacteria from the distal ileum throughout the colon can effectively increase SCFA production, specifically butyrate, which is not only the preferred energy source for colonocytes, but increases epithelial cell proliferation, trophic growth of the intestinal mucosa, and increased transmural intestinal resistance (D'Argenio et al., 1996; Mariadason et al., 1997; Inan et al., 2000). Several researchers have demonstrated the fermentability and prebiotic capabilities of dietary fibers, such as fructans (scFOS and inulin) and their ability to stimulate beneficial bacteria, such as *Lactobacillus* and *Bifidobacteria*, increase production of SCFA, and reduce intestinal permeability (Grizard & Barthomeuf, 1999; Bouhnik et al., 2007; Hernot et al., 2009). This evidence led to our investigation to study the effects of fructan prebiotics (scFOS and inulin) on intestinal resistance, histomorphology, and gene expression in the gastrointestinal tract.

In examining the characteristics of these fructan prebiotics, Roberfroid et al. (1998) reported that *in vitro* fermentation of fructans with greater than 10 DP are fermented slower than lower DP fructans. Complementary to this work, Stewart et al. (2008) also found FOS containing DP <10 was quickly fermented in an *in vitro* model, whereas inulin (DP >20) was steadily fermented, which was depicted by time and SCFA production. Therefore, in light of this evidence, we hypothesized that scFOS would be rapidly fermented due to their low DP. Therefore, intestinal architecture and resistance would improve in the distal ileum and cecum, whereas inulin would be fermented at a slower rate and would have moderate effects on all regions of the hindgut.

We demonstrated that fructan supplementation increased ileal and cecal crypt depth, the regions where most fermentative activity likely occurred. Kleessen et al. (2003) reported that human-flora associated rats (germ-free rats inoculated with human microflora) fed a mixture of oligofructose and long-chain inulin had longer jejunal villi and greater crypt depth in the distal

colon. This information may reveal a potential benefit to a change in intestinal architecture upon prebiotic supplementation. To support this notion, Yason et al. (1987) and Hedemann et al. (2003) reported greater crypt depth as a response to increased epithelial cell turnover. This increased proliferation may subsequently lead to increased absorptive capabilities at the villus surface (Yason et al., 1987; Awad et al., 2011). In relation to these findings, Benjamin et al. (2000) reported that increased epithelial cell proliferation caused narrowing and reduced width of epithelial cells, which was associated with increased intestinal resistance. However, 10% cellulose-fed mice also had substantially deeper crypts in the distal colon compared to 10% scFOS-fed mice in this current study, which may suggest benefits of insoluble fiber in the hindgut. In contrast, soluble fibers may yield benefits to the proximal gut. Collectively, these data show a possible benefit to including a combination of insoluble and soluble fibers in the diet.

Our data also demonstrated that scFOS and inulin increased transmural resistance compared to the 5% cellulose control group, with the highest resistance values occurring in the cecum and distal colon. In agreement with our findings of improved intestinal resistance upon prebiotic supplementation, Cani et al. (2009) also reported increased intestinal resistance in obese mice supplemented with 10% oligofructose compared to standard chow fed mice. However, because the transmural resistance data of mice fed 10% cellulose were not significantly different from those fed the fructan treatments in the current study, this would suggest a concentration effect of specific dietary fibers rather than a solubility or fermentability effect. Yet, to better understand the mechanisms by which intestinal resistance was improved after prebiotic supplementation, other than mechanisms demonstrated by Benjamin et al. (2000), as mentioned previously, we assessed the expression (mRNA abundance) of many genes that

may be involved with increased fermentation, SCFA production, and consequent improvements in intestinal function. We hypothesized that the expression of SCFA transporters, tight junction proteins, AMPK, and MUC2 would be positively correlated with intestinal barrier resistance.

In the present study, the main effect of diet had no significant effects on SCFA transporter and receptor mRNA abundance. This may suggest activation of these transporters, regardless of the type of fermentable substrate within these regions. Given the previous literature on prebiotics and the response observed in histomorphology and resistance herein, however, other reasons for no change seem more likely. It is possible that these transporters are not regulated at the mRNA level or are regulated by more than SCFA alone. SCFA transporters may also be involved in transport of other fermentation by-products, such as lactate. Lastly, the localization of these transporters could also play a role in SCFA or other by-product up-regulation. Kirat & Kato (2000) used immunofluorescence images to show that the presence of MCT-1 was predominately concentrated at the basolateral crypt of the cecum, proximal colon, and distal colon of rumen models (Kirat & Kato, 2006). These authors further theorized that the entry of SCFA into the cell is caused by the diffusion of a protonated SCFA and transporters coupled with bicarbonate ions to transport deprotonated SCFA (Kirat & Kato, 2006).

The protein adhesions of the tight junction complex, occludin and ZO-1, are very important in maintaining the resistance of the intestinal barrier. For example, Al-Sadi et al. (2011) reported that the selective knockout of occludin from Caco-2 monolayers and in mice caused increased transepithelial flux of macromolecules, such as mannitol, inulin, and dextran. Cani et al. (2009) reported increased intestinal ZO-1 expression in obese mice after oligofructose supplementation, which was also associated with decreased intestinal permeability. We observed a decrease in ZO-1 expression in the distal colon of inulin-fed mice, which was not expected due

to evidence showing steady fermentation of inulin and possible ability to reach the hindgut. The results for occludin expression were not exactly as expected either. Occludin acts as a bridge between adjacent epithelial cells. Therefore, increased expression of occludin may strengthen the bond between these cells while remaining firmly anchored to ZO-1 proteins located in the peripheral membrane of these cells (Groschwitz & Hogan, 2009). We did not expect the expression of occludin to be decreased in the hindgut of mice fed inulin or scFOS, but that is what was observed in the proximal and distal colon of the current study. We hypothesized that increased SCFA production would increase occludin expression. It is possible, however, that other mechanisms were involved. Stimulation may have been due to the nondigestible and bulky material provided in the form of cellulose, and the expansion of the colon that may have occurred, increasing the physical pressure on the tight junction complex within the colon.

The expression of AMPK was assessed due to the growing evidence of its involvement in intestinal barrier maintenance. We found AMPK to be elevated in the cecum of 10% scFOS-fed mice, which was to be expected due to the high fermentative capacity. Peng et al. (2009) demonstrated the involvement of AMPK in regulating tight junction proteins and restoration of intestinal resistance. In that study, Caco-2 cell monolayers underwent calcium-switch procedures to cause limited relocation of occludin and ZO-1 to the tight junction complex. However, the addition of butyrate to the medium caused the majority of ZO-1 proteins to re-localize to the tight junction complex. Yet, when AMPK was inhibited in this medium, the addition of butyrate did not re-localize ZO-1 to the tight junction matrix and intestinal barrier function declined. This evidence may indicate that butyrate activates AMPK and, thus, accelerates the repair of damaged tight junction complexes. Scharl et al. (2009) also reported the involvement of AMPK in intestinal permeability. T84 intestinal epithelial cells incubated for 6 h with IFN-γ increased

AMPK activation by 44% more than controls, which also was associated with decreased occludin expression. Our data showed a decline in occludin expression in prebiotic-supplemented mice; however, this decline in expression occurred predominantly in the colon segments. This may also suggest the exhaustion of fermentative substrates and lack of dietary fiber, in general, before reaching the colon segments, limiting the expression of occludin to distal intestinal segments. MCT-1 expression was positively correlated to the expression of AMPK, ZO-1, and occludin in the distal colon of our mouse model, which may suggest the involvement of these variables working together to benefit intestinal resistance. Proximal colon crypt depth was also correlated with AMPK, which may suggest that a change in intestinal architecture may positively influence intestinal resistance.

Because the colon has a dense community of bacteria, the mucus layer has an important role in the protection against adhesive and invasive species of intestinal microbiota (Atuma et al., 2001; Corazziari, 2009). It is well known that the mucus layer increases from the proximal to the distal regions of the gut (Kleessen et al., 2003; Corazziari, 2009). We proposed that increased mucin production may increase the thickness of the mucous layer in the gut and subsequently increase intestinal barrier function. Overall, expression of MUC2 was greater in the proximal and distal colon, but was not statistically significant. However, we observed a moderate correlation ($R^2 = 0.4$) between ileal transmural resistance and ileal MUC2 expression, indicating a possible relationship between these variables, but actual depth of the intestinal mucus layer was not measured in this study.

As stated, the importance of the intestinal barrier cannot be overlooked and, therefore, generates concern about the increased intestinal permeability noted in the metabolic dysfunctional state of obesity. Fructan prebiotics have shown promise in rectifying this problem.

Our study showed that intestinal transmural resistance improves with prebiotic supplementation, regardless of DP, in an obese mouse model. However, we also found higher concentrations of cellulose may have equivalent benefits throughout the gut or in specific regions, such as the colon. These data suggest that feeding a combination of both soluble and insoluble fibers may benefit the full length of the intestine, wherein, fructans have more immediate effects in the ileum and cecum, while cellulose-based fibers have beneficial effects in the distal regions of the colon.

The nature of gene involvement in intestinal barrier maintenance is unclear, but our evidence identifies the regional expression of these markers and, therefore, contributes to the growing body of evidence regarding the involvement of prebiotic and cellulose fibers in intestinal barrier function and gut health.

Literature Cited

Al-Sadi, R., Khatib, K., Guo, S., Ye, D., Youssef, M., & Ma, T. (2011). Occludin regulates macromolecules flux across the intestinal epithelial tight junction barrier. *Am. J. Physiol. Gastrointest. Liver Physiol*., 300, G1054-1064.

Atuma, C., Strugala, V., Allen, A., & Holm, L. (2001). The adherent gastrointestinal mucus gel layer: Thickness and physical state in vivo. *Am. J. Physiol. Gastrointest. Liver Physiol., 280*, G922-G929.

Awad, W. A., Ghareeb, K., & Bohm, J. (2010). Evaluation of the chicory inulin efficacy on ameliorating the intestinal morphology and modulating the intestinal electrophysiological properties in broiler chickens. *J. Anim. Physiol. Anim. Nutr., 95*, 65-72.

Barbier de La Serre, C., Ellis, C. L., Lee, J., Hartman, A. L., Rutledge, J. C., & Raybould, H. E. (2010). Propensity to high fat diet-induced obesity in rats is associated with changes in the gut microbiota and gut inflammation. *Am. J. Physiol. Gastrointest. Liver Physiol., 10*, G440-G448.

Benjamin, M. A., McKay, D. M., Yang, P. C., Cameron, H., & Perdue, M. H. (2000). Glucagon-like peptide-2 enhances intestinal epithelial barrier function of both transcellular and paracellular pathways in the mouse. *Gut, 47*, 112-119.

Bouhnik, Y., Achour, L., Paineau, D., Riottot, M., Attar, A., & Bornet, F. (2007). Four-week short chain fructo-oligosaccharides ingestion leads to increasing fecal bifidobacteria and cholesterol excretion in healthy elderly volunteers. *Nutr. J., 6*, 42-49.

Brun, P., Castagliuolo, I., Di Leo, V., Buda, A., Pinzani, M., Palu, G., & Martines, D. (2007). Increased intestinal permeability in obese mice: new evidence in the pathogenesis of nonalcoholic steatohepatitis. *Am. J. Physiol. Gastrointest. Liver Physiol., 292*, G518-G525.

Cani, P. D., Possemiers, S., Van de Wiele, T., Guiot, Y., Everard, A., Rottier, O., Geurts, L., Naslain, D., Neyrinck, A., Lambert, D., Muccioli, G., & Delzenne, N. (2009). Changes in gut microbiota control inflammation in obese mice through a mechanism involving GLP-2-driven improvement of gut permeability. *Gut, 58*, 1091-1103.

Corazziari, E. S. (2009). Intestinal mucus barrier in normal and inflamed colon. *J. Pediatr. Gastroenterol. Nutr., 48*, S54-S55.

D'Argenio, G., Cosenza, V., Delle, C. M., Iovino, P., Delle, V. N., Lombardi, G., & Mazzacca, G. (1996). Butyrate enemas in experimental colitis and protection against large bowel cancer in a rat model. *Gastroenterol., 110*, 1727-1734.

Gardiner, K. R., Halliday, M. I., Barclay, G. R., Milne, L., Brown, D., Stephens, S., Maxwell, R., & Rowlands, B. (1995). Significance of systemic endotoxaemia in inflammatory bowel disease. *Gut, 36*, 897-901.

Grizard, D., & Barthomeuf, C. (1999). Non-digestible oligosaccharides used as prebiotic agents: Mode of production and beneficial effects on animal and human health. *Reprod. Nutr. Dev., 39*, 563-588.

Groschwitz, K. R., & Hogan, S. P. (2009). Intestinal barrier function: Molecular regulation and disease pathogenesis. *J. Allergy Clin. Immunol., 124*, 3 - 14.

Halestrap, A. P., & Price, N. T. (1999). The proton-linked monocarboxylate transporter (MCT) family: Structure, function, and regulation. *Biochem. J., 343*, 281-299.

Hernot, D. C., Boileau, T. W., Bauer, L. L., Middelbos, I. S., Murphy, M. R., Swanson, K. S., & Fahey, G.C., Jr. (2009). In vitro fermentation profiles, gas production rates, and microbiota modulation as affected by certain fructans, galactooligosaccharides, and polydextrose. *J. Agric. Food Chem., 57*, 1354-1361.

Hollander, D., Vadheim, C. M., Brettholz, E., Petersen, G. M., Delahunty, T., & Rotter, J. I. (1986). Increased intestinal permeability in patients with Crohn's disease and their relatives. A possible etiologic factor. *Ann. Intern. Med., 105*, 883-885.

Huber, W., Herrmann, G., Schuster, T., Phillip, V., Saugel, B., Schultheiss, C., Hoellthaler, J., Gaa, J., Hartel, M., Schmid, R., & Reindl, W. (2010). Life-threatening complications of Crohn's disease and ulcerative colitis: A systematic analysis of admissions to an ICU during 18 years. *Dtsch. Med. Wochenschr., 135*, 668-674.

Inan, M. S., Rasoulpour, R. J., Yin, L., Hubbard, A. K., Rosenberg, D. W., & Giardina, C. (2000). The luminal short-chain fatty acid butyrate modulates NF-κB activity in a human colonic epithelial cell line. *Gastroenterol., 118*, 724-734.

Kleessen, B., Hartmann, L., & Blaut, M. (2003). Fructans in the diet cause alterations of intestinal mucosal architecture, released mucins and mucosa-associated bifidobacteria in gnotobiotic rats. *Br. J. Nutr., 89*, 597-606.

Leser, T., & Molbak, L. (2009). Better living through microbial action: the benefits of the mammalian gastrointestinal microbiota on the host. *Environ. Microbiol., 11*, 2194-2206.

Laukoetter, M., Nava, P., Lee, W., Severson, E., Capaldo, C., Babbin, B., Williams, I., Koval, M., Peatman, E., Campbell, J., Dermody, T., Nusrat, A., & Parkos, C. (2007). JAM-A regulates permeability and inflammation in the intestine in vivo. *J. Exp. Med., 204*, 3067-3076.

Macfarlene, S., & Macfarlene, G. T. (2003). Regulation of short-chain fatty acid production. *Proc. Nutr. Soc. , 62*, 67-72.

Mariadason, J., Barkla, D., & Gibson, P. (1997). Effect of short-chain fatty acids on paracellular permeability in Caco-2 intestinal epithelium model. *Am. J. Physiol., 272*, G705-G712.

Peng, L., Li, Z. -R., Green, R. S., Holzman, I. R., & Lin, J. (2009). Butyrate enhances the intestinal barrier by facilitating tight junction assembly via activation of AMP-activated protein kinase in Caco-2 cell monolayers. *J. Nutr., 139*, 1619-1625.

Physiological data summary (2007, December 13). Retrieved February 15, 2012, from The Jackson Laboratory: http://jaxmice.jax.org/support/phenotyping/B6data000664.pdf

Roberfroid, M. B., Van Loo, J. A., & Gibson, G. R. (1998). The bifidogenic nature of chicory inulin and its hydrolysis products. *J. Nutr., 128*, 11-19.

Roberfroid, M., Gibson, G. R., Hoyles, L., McCartney, A. L., Rastall, R., Rowland, R., Wolvers, D., Watzl, B., Szajewska, H., Stahl, B., Guarner, F., Respondek, F., Whelan, K., Coxam, V., Davicco, M., Léotoing, L., Wittrant, Y., Delzenne, N., Cani, P., Neyrinck, A., & Meheust, A. (2010). Prebiotic effects: metabolic and health benefits. *Br. J. Nutr., 104*, S3 - S51.

Scharl, M., Paul, G., Barrett, K. E., & McCole, D. F. (2009). AMP-activated protein kinase mediates the interferon-γ-induced decrease in intestinal epithelial barrier function. *J. Biol. Chem., 284*, 27952-27963.

Yason, C., Summers, B., & Schat, K. (1987). Pathogenesis of rotavirus infection in various age groups of chickens and turkeys: pathology. *Am. J. Vet. Res., 48*, 927-938.

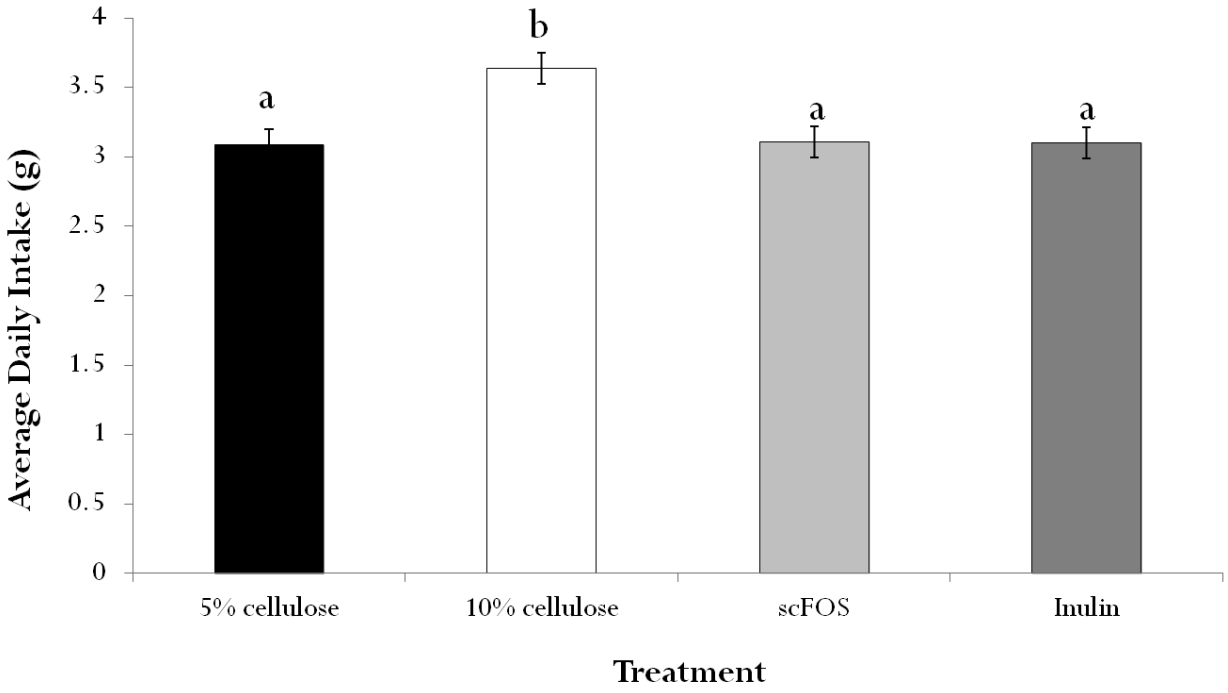

Figure 3.1 Average daily food intake of C57BL/6 mice (n=6). Means lacking a common superscript letter differ ($p<0.05$).

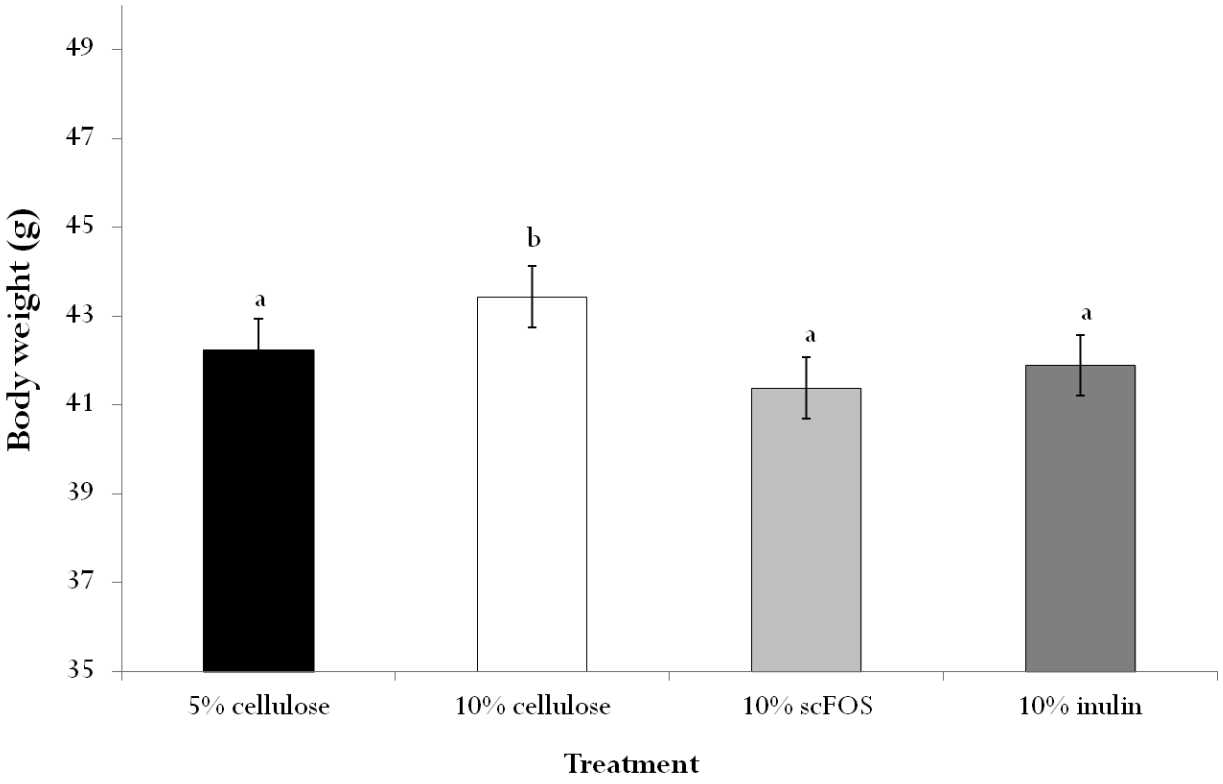

Figure 3.2 Body weight of C57BL/6 mice (n=6) at 24-wk. Means lacking a common superscript letter differ ($p<0.01$).

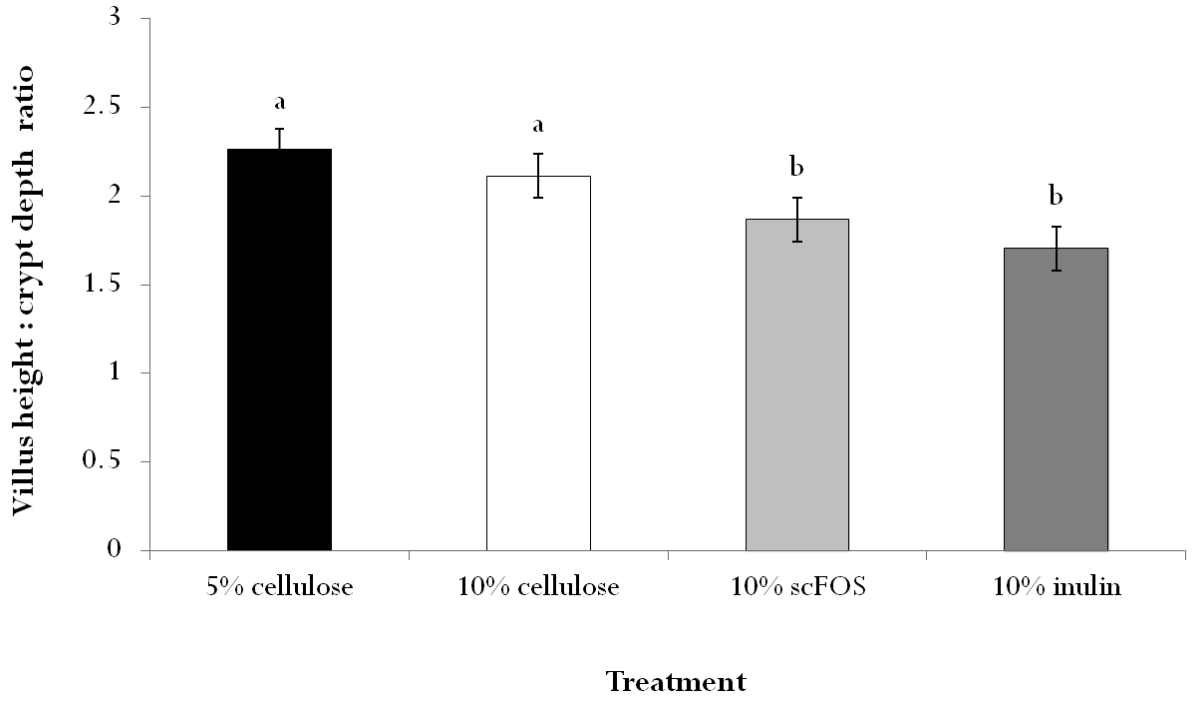

Figure 3.3 Ileal villus height: crypt depth ratios in C57BL/6 mice (n=6). Means lacking a common superscript letter differ ($p<0.05$).

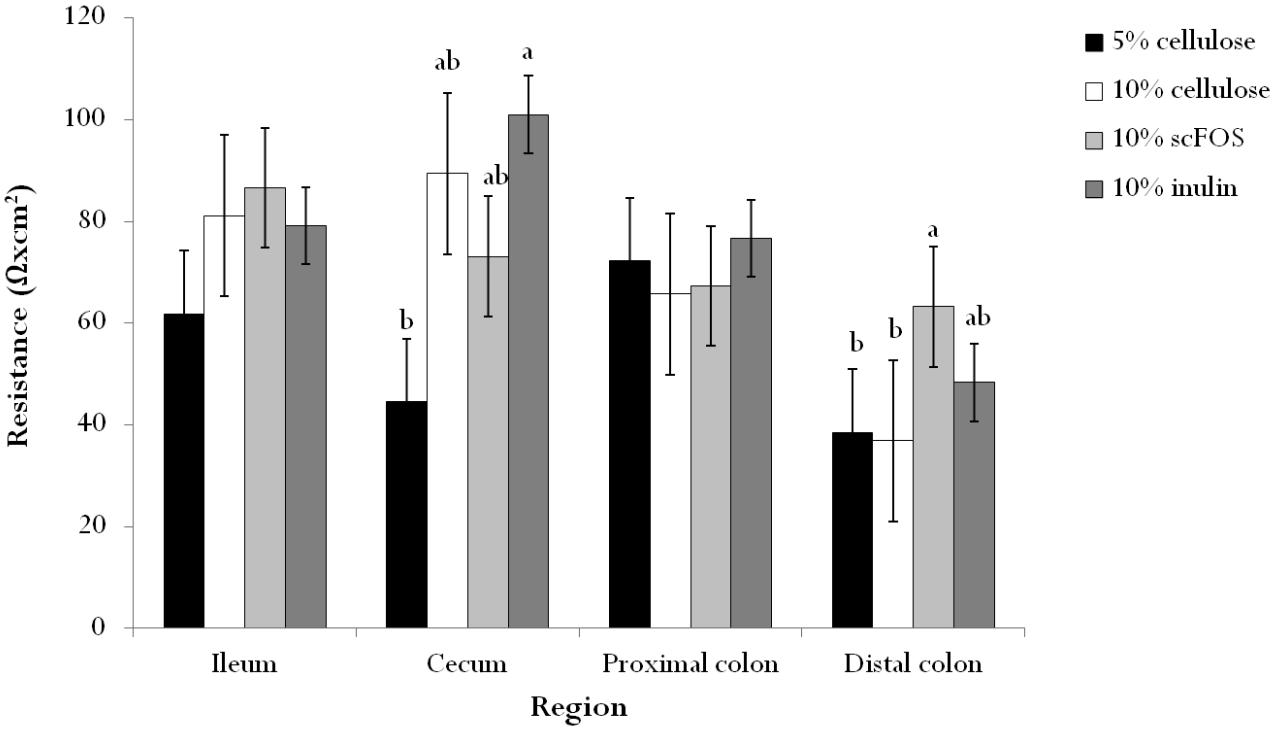

Figure 3.4 Transmural resistance in the ileum, cecum, proximal colon, and distal colon of C57BL/6 mice (n=6). Means lacking a common superscript letter differ ($p<0.05$).

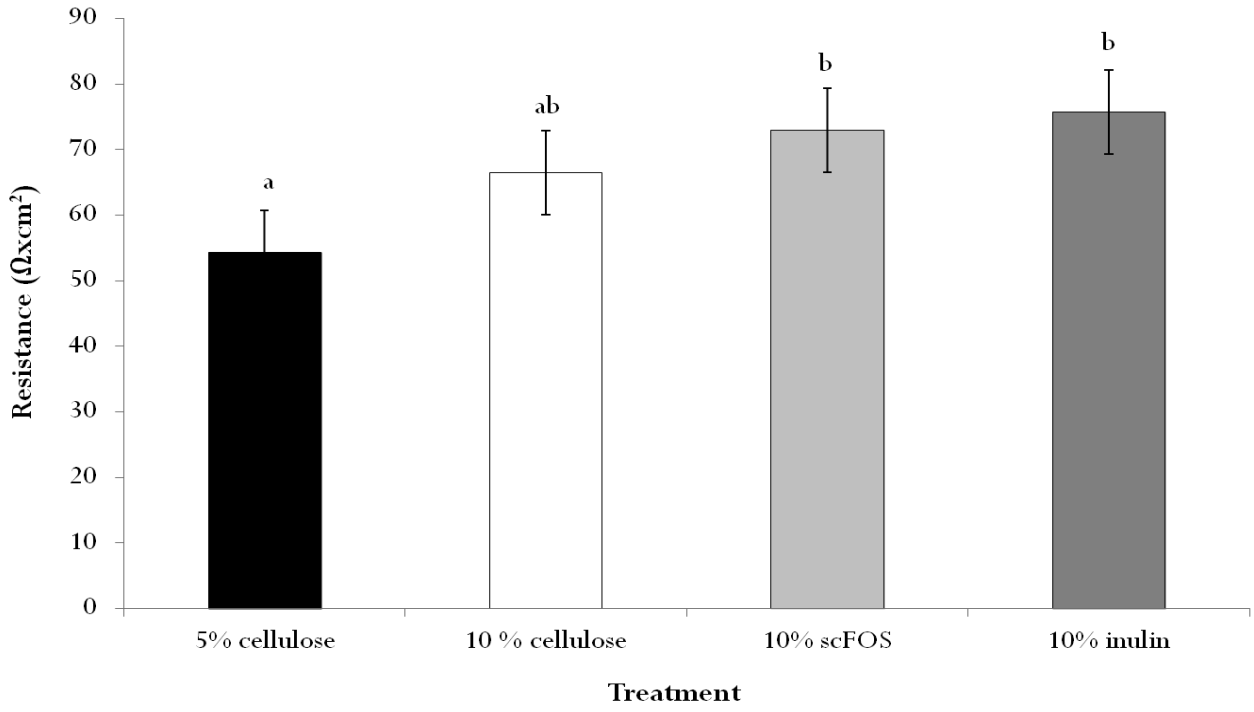

Figure 3.5 Main effect of diet on transmural resistance among regions in C57BL/6 mice (n=6). Means lacking a common superscript letter differ ($p<0.05$).

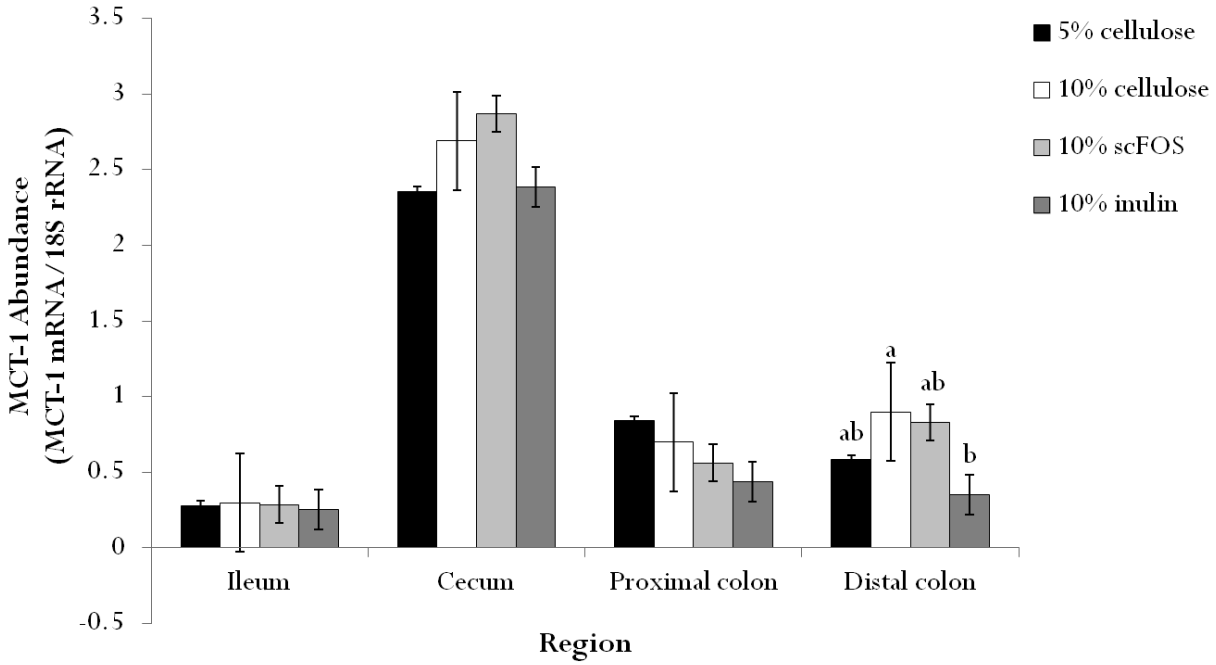

Figure 3.6 MCT-1 mRNA abundance in the ileum, cecum, proximal colon, and distal colon of C57BL/6 mice (n=6). Means lacking a common superscript letter differ ($p<0.05$).

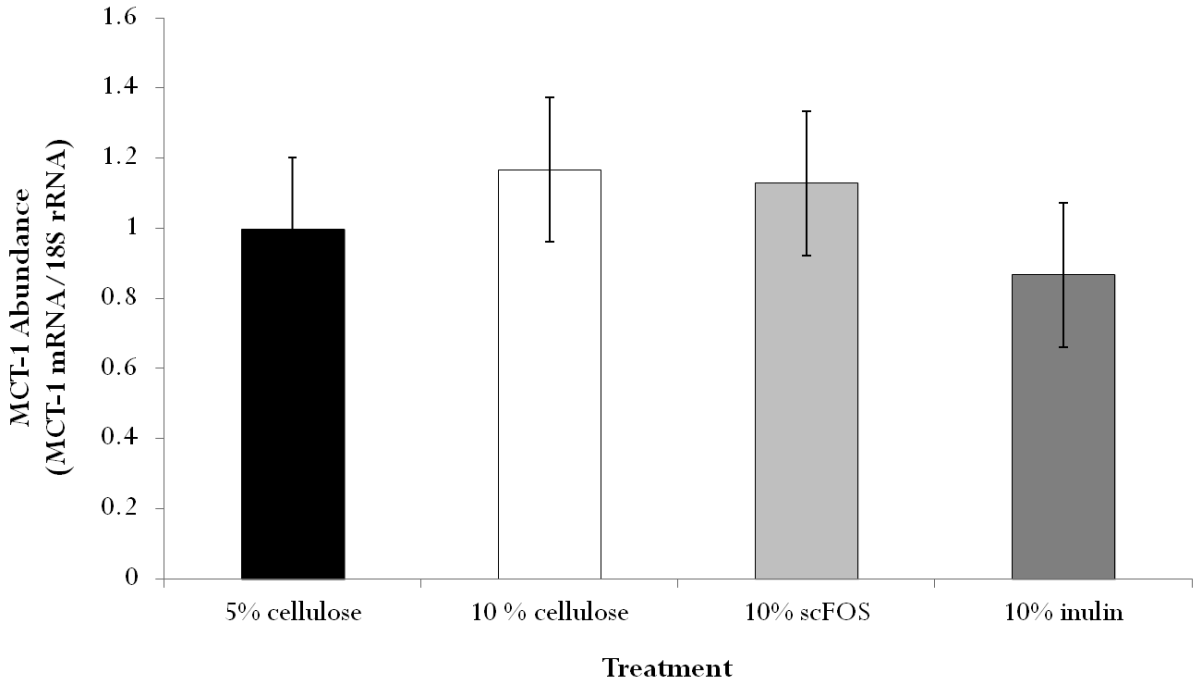

Figure 3.7 Main effect of diet on MCT-1 mRNA abundance among regions in C57BL/6 mice (n=6).

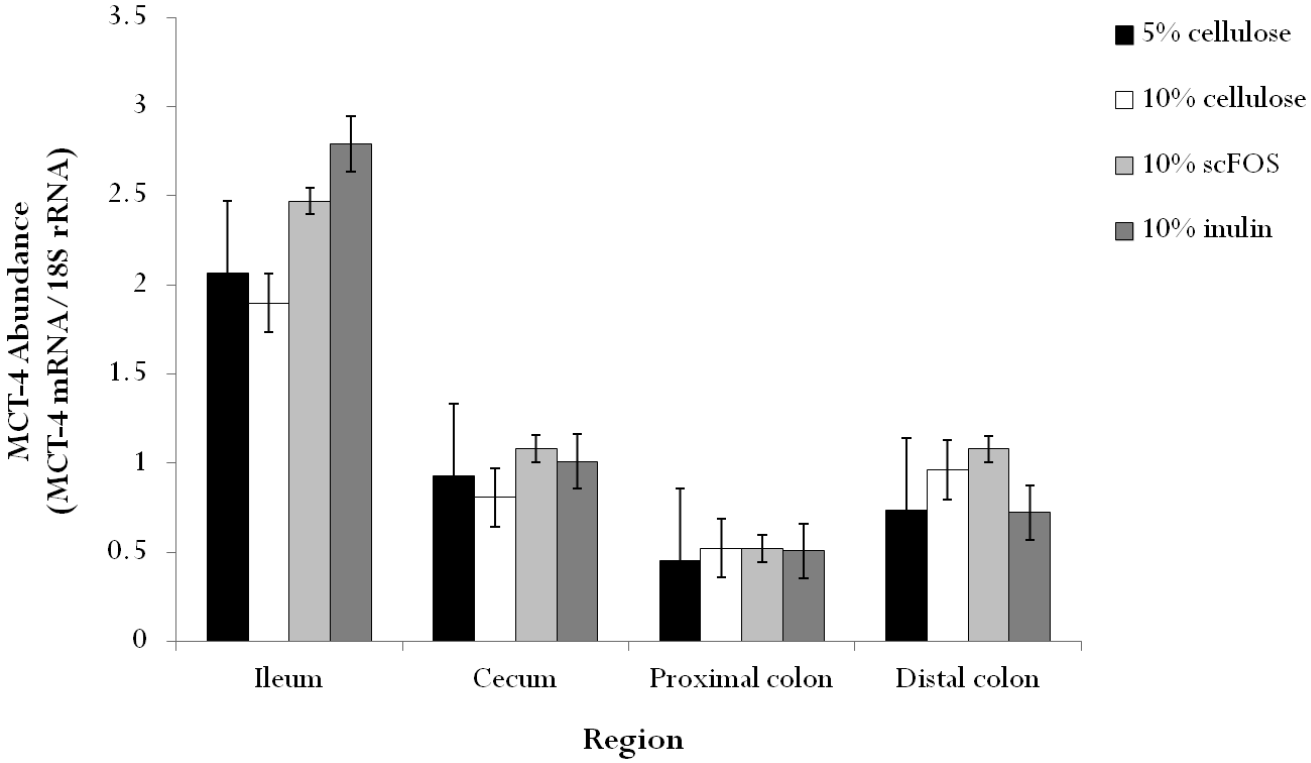

Figure 3.8 MCT-4 mRNA abundance in the ileum, cecum, proximal colon, and distal colon of C57BL/6 mice (n=6).

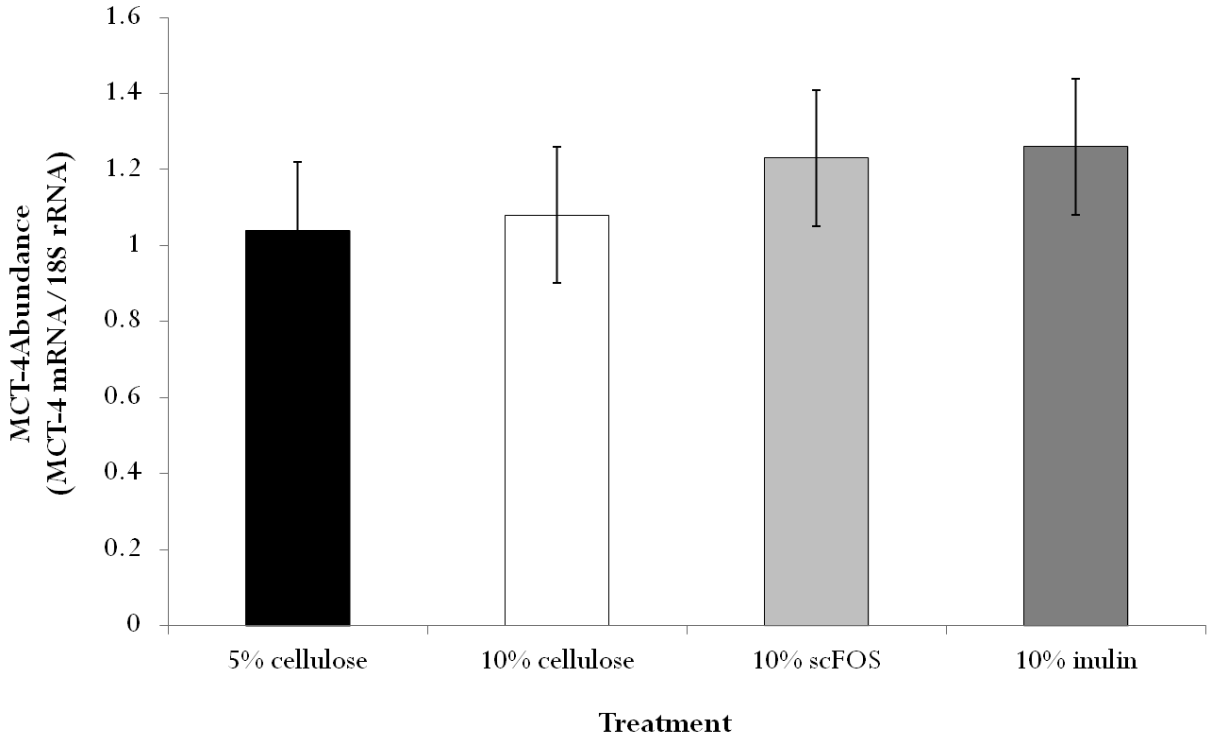

Figure 3.9 Main effect of diet on MCT-4 mRNA abundance among regions in C57BL/6 mice (n=6).

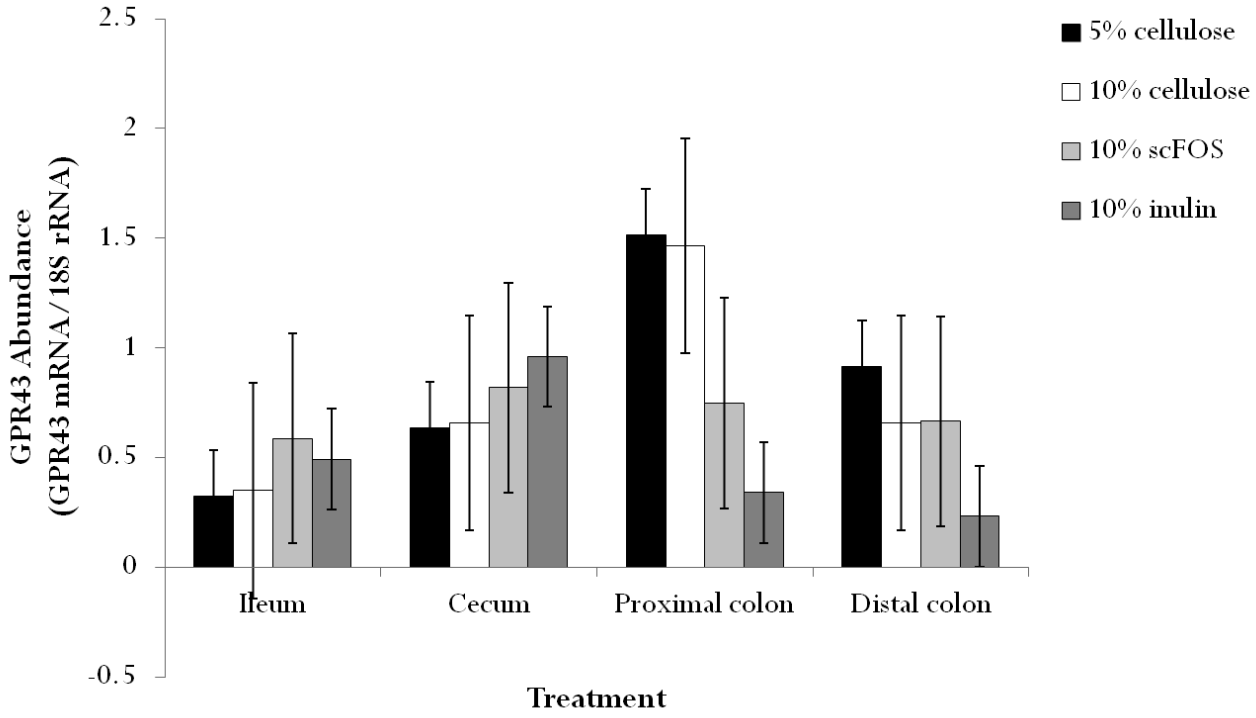

Figure 3.10 GPR43 mRNA abundance in the ileum, cecum, proximal colon, and distal colon of C57BL/6 mice (n=6).

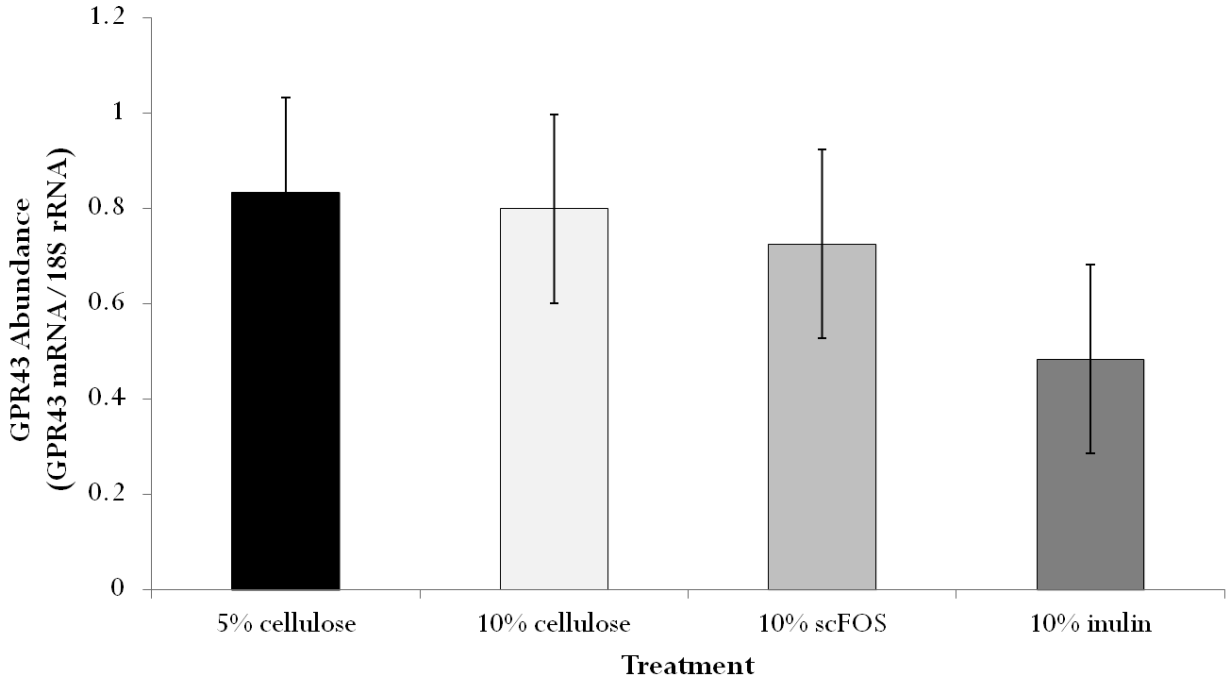

Figure 3.11 Main effect of diet on GPR43 mRNA abundance among regions in C57BL/6 mice (n=6).

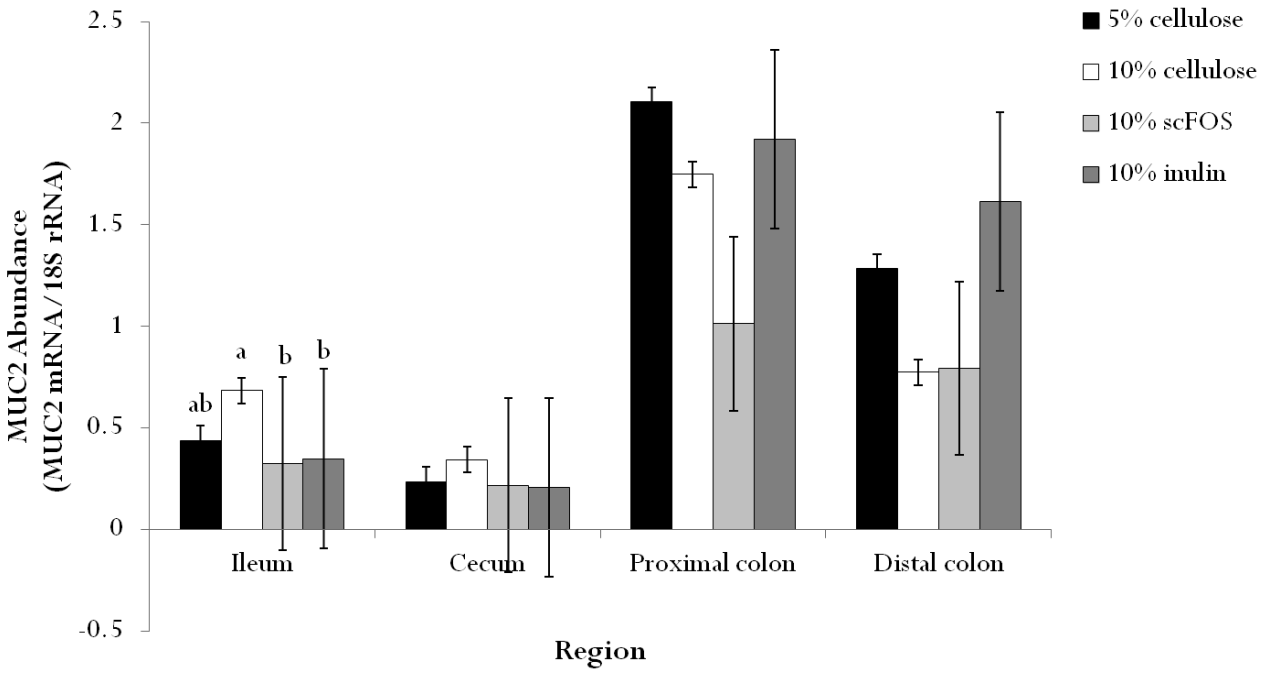

Figure 3.12 MUC2 mRNA abundance in the ileum, cecum, proximal colon, and distal colon of C57BL/6 mice (n=6). Means lacking a common superscript letter differ ($p<0.05$).

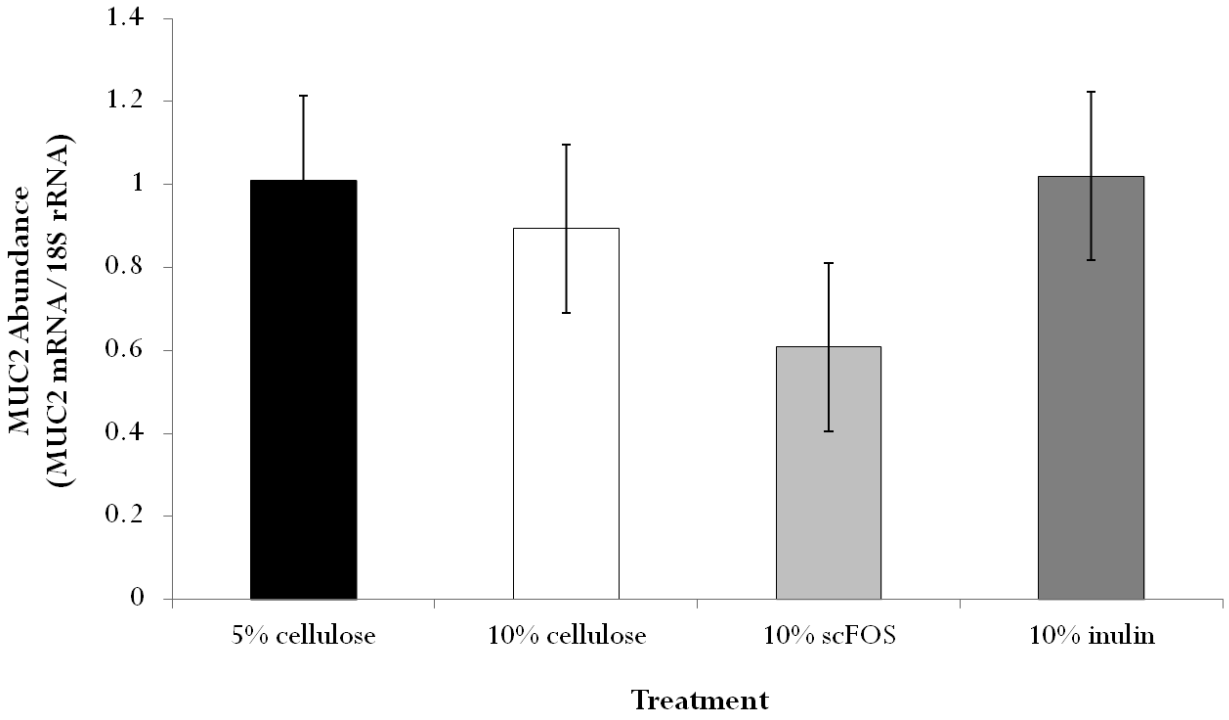

Figure 3.13 Main effect of diet on MUC2 mRNA abundance among regions in C57BL/6 mice (n=6).

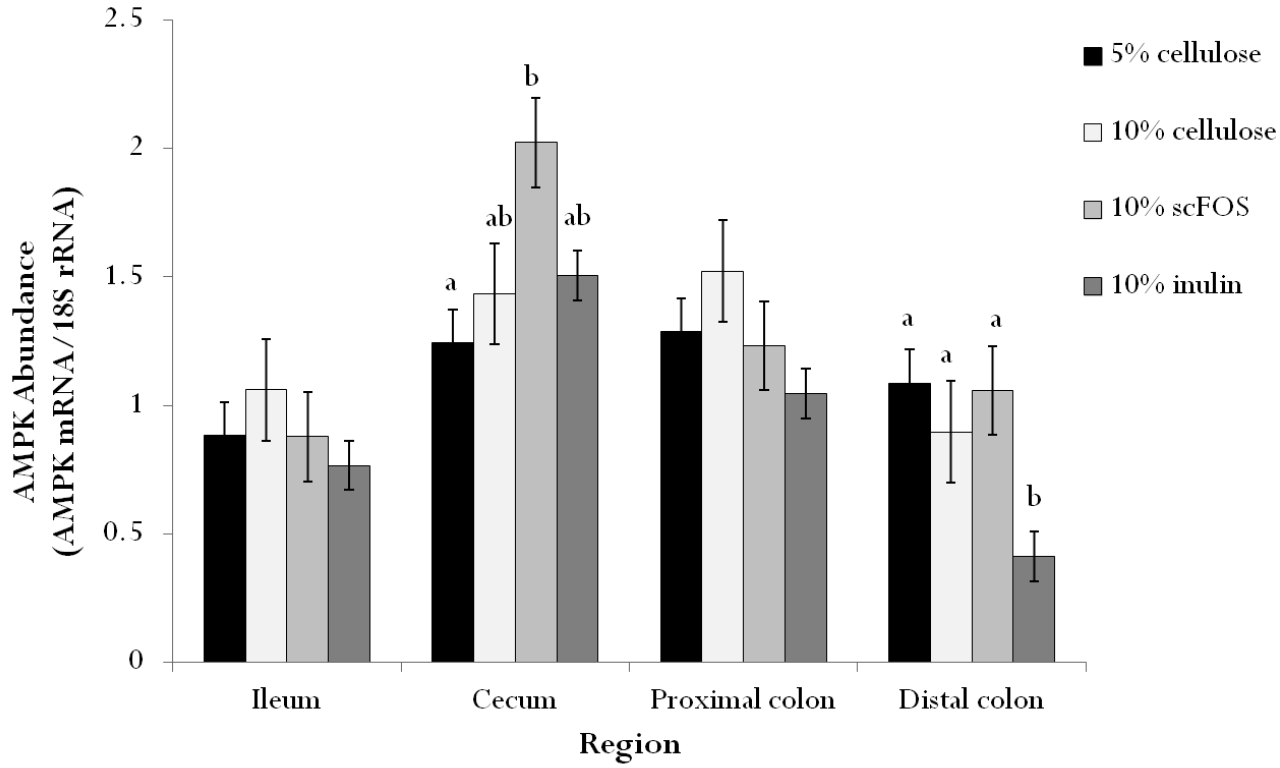

Figure 3.14 AMPK mRNA abundance in the ileum, cecum, proximal colon, and distal colon of C57BL/6 mice (n=6). Means lacking a common superscript letter differ ($p<0.05$).

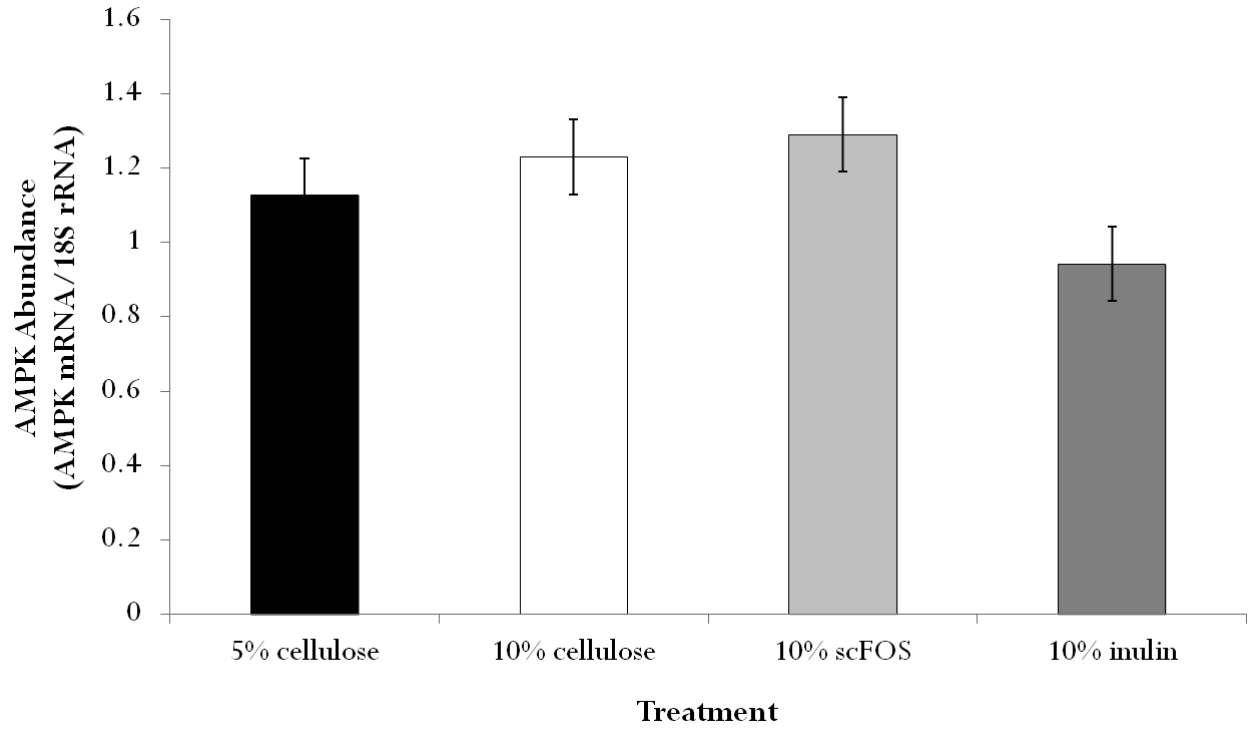

Figure 3.15 Main effect of diet on AMPK mRNA abundance among regions in C57BL/6 mice (n=6).

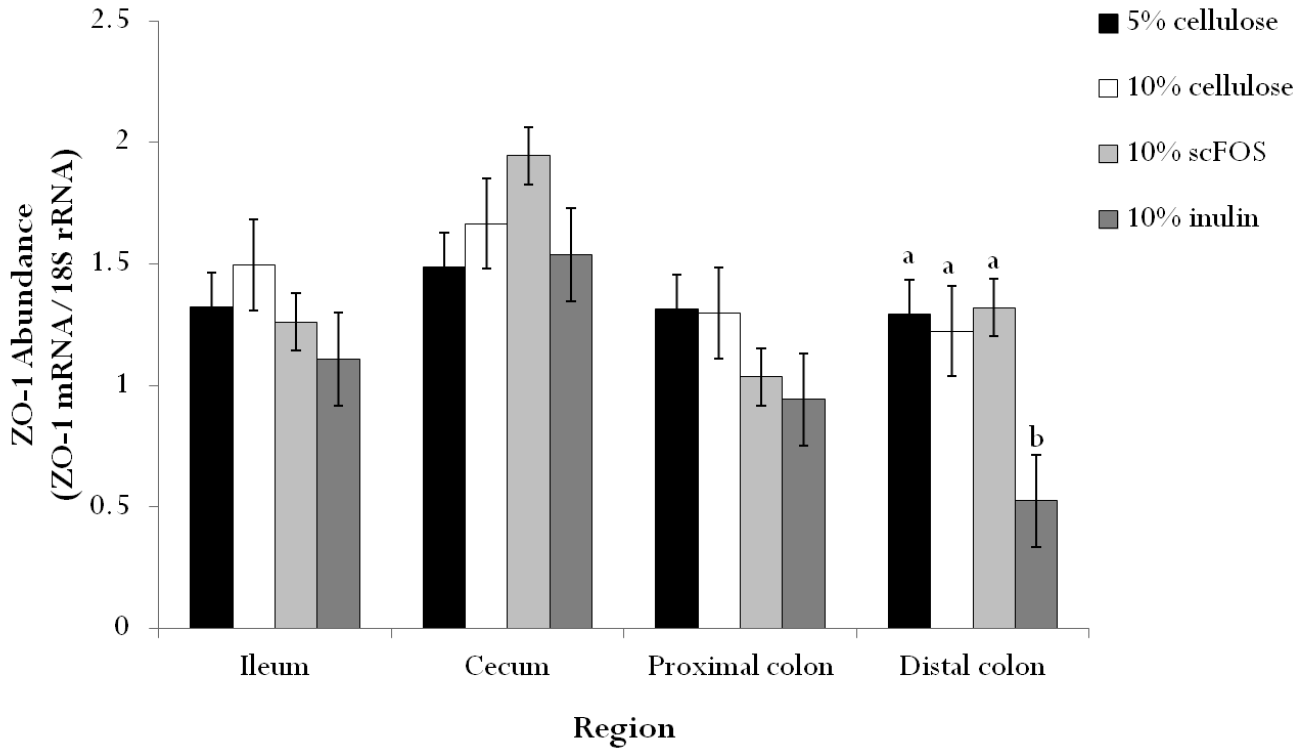

Figure 3.16 ZO-1 mRNA abundance in the ileum, cecum, proximal colon, and distal colon of C57BL/6 mice (n=6). Means lacking a common superscript letter differ ($p<0.05$).

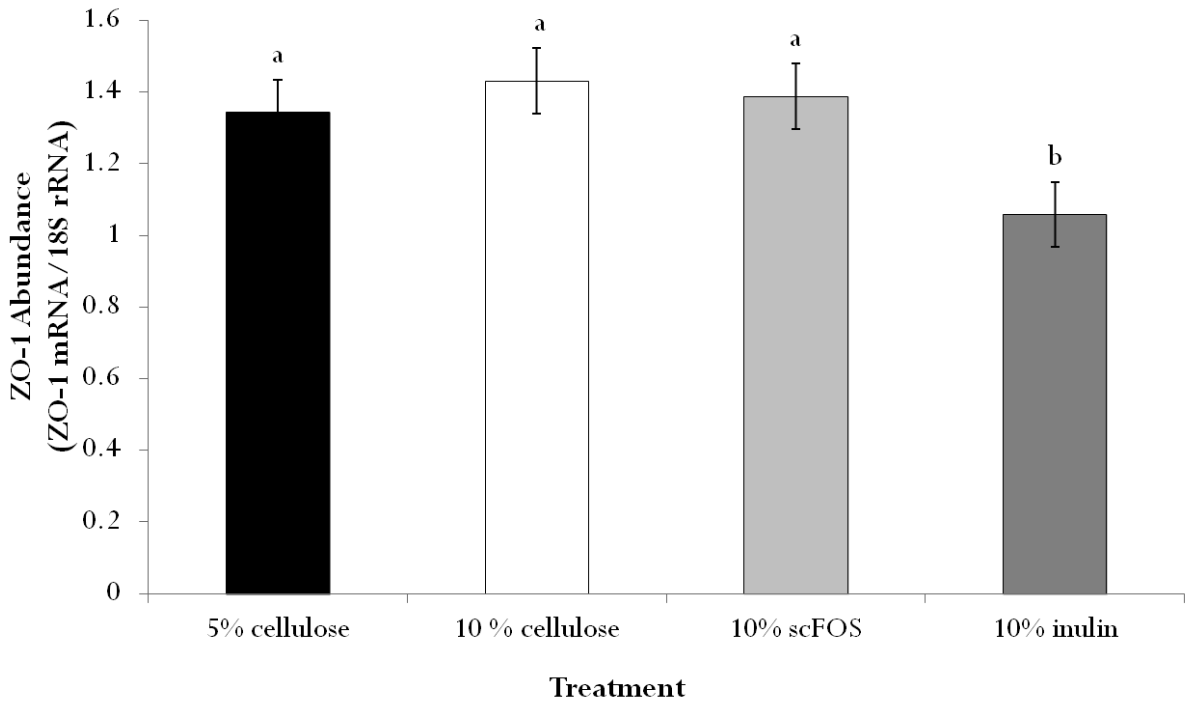

Figure 3.17 Main effect of diet on ZO-1 mRNA abundance in C57BL/6 mice (n=6). Means lacking a common superscript letter differ ($p<0.05$).

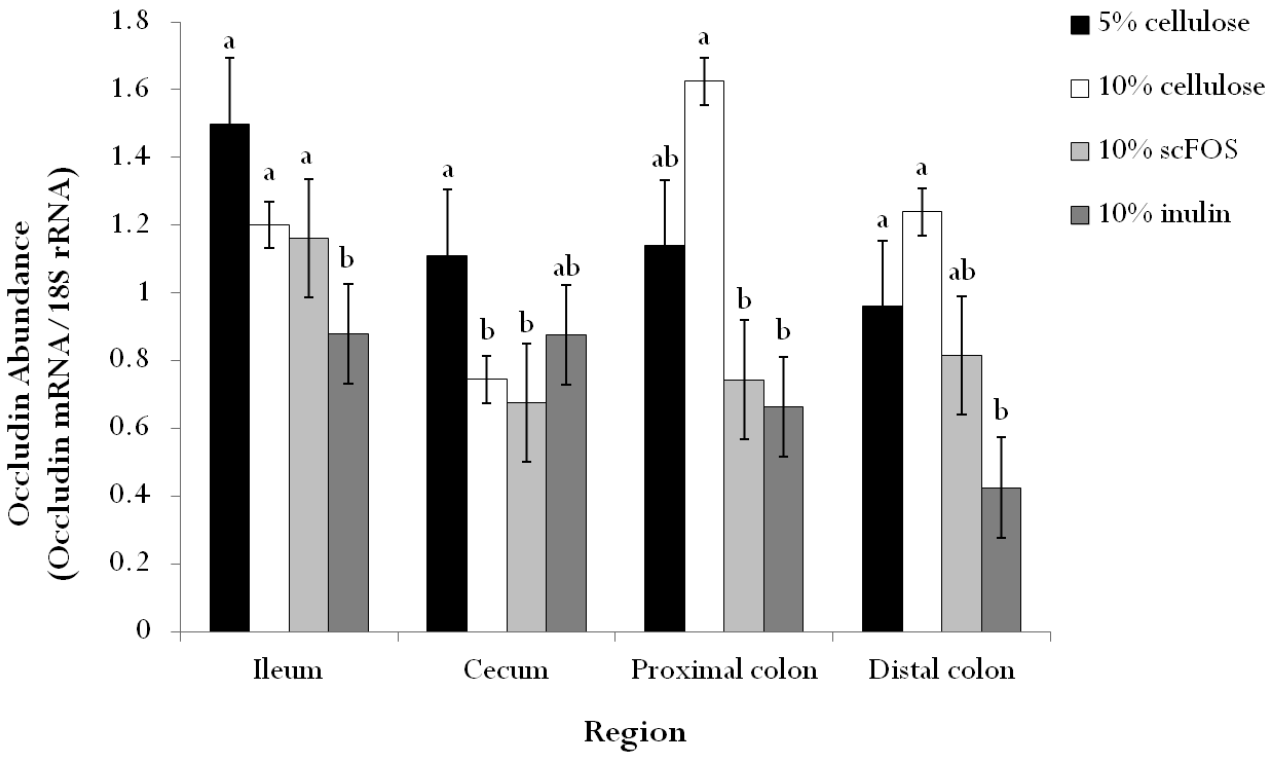

Figure 3.18 Occludin mRNA abundance in the ileum, cecum, proximal colon, and distal colon of C57BL/6 mice (n=6). Means lacking a common superscript letter differ ($p<0.05$).

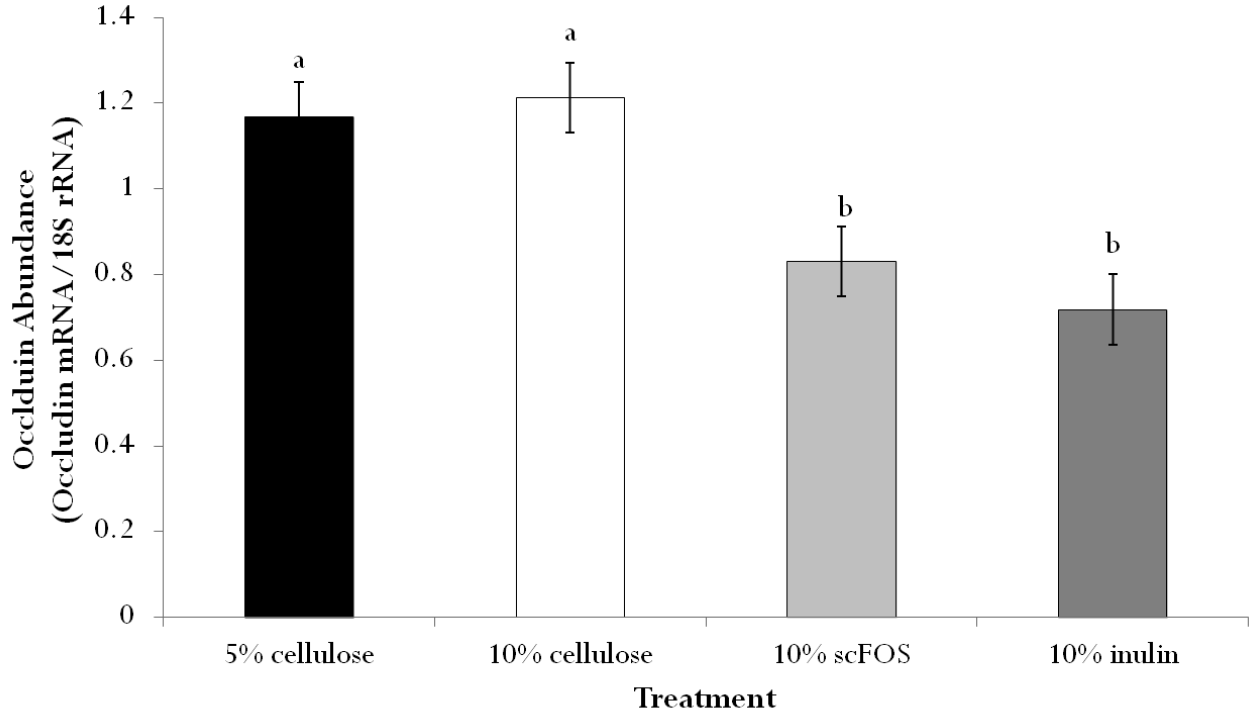

Figure 3.19 Main effect of diet on occludin mRNA abundance among regions in C57BL/6 mice (n=6). Means lacking a common superscript letter differ ($p<0.05$).

Table 3.1 Ingredient composition of pelleted AIN-93G diets containing 45% kilocalories as fat and either non-fermentable dietary fiber or fructan prebiotics (g/kg)

Ingredient	5% cellulose	10% cellulose	10% inulin	10% scFOS
Casein, 80 mesh	233.1	220.2	220.2	220.2
L-cystine	3.5	3.3	3.3	3.3
Cornstarch	84.8	80.2	80.2	80.2
Maltodextrin	116.5	110.1	110.1	110.1
Sucrose	201.4	190.3	190.3	190.3
Cellulose	58.3	110.1	0.0	0.0
Inulin	0.0	0.0	110.1	0.0
Fructooligosaccharides	0.0	0.0	0.0	110.1
Soybean oil	29.1	27.5	27.5	27.5
Lard	206.8	195.5	195.5	195.5
Mineral mix[1]	52.4	52.4	52.4	52.4
Vitamin mix[2]	11.7	11.7	11.7	11.7
Choline bitartrate	2.3	2.3	2.3	2.3

[1] **Mineral mix consists of: calcium carbonate anhydrous (357 g), potassium phosphate monobasic (196 g), potassium citrate, tripotassium monohydrate (70.78 g), sodium chloride (74 g), potassium sulfate (46.60 g), magnesium oxide (24 g), ferric citrate (6.06 g), zinc carbonate (1.65 g), sodium meta-silicate-9H_2O (1.45 g), manganous carbonate (0.63 g), cupric carbonate (0.30 g), chromium potassium sulfate-12H_2O (0.28 g), boric acid (81.5 mg), sodium fluoride (63.5 mg), nickel carbonate (31.8 mg), lithium chloride (17.4 mg), sodium selenate anhydrous (10.25 mg), potassium iodate (10 mg), ammonium paramolybdate-4H_2O (7.95 mg), and ammonium vanadate (6.6 mg).**

[2]**Vitamin mix consists of: nicotinic acid (3 g), calcium pantothenate (1.60 g), pyridoxine-HCl (0.70 g), thiamin-HCl (0.60 g), riboflavin (0.60 g), folic acid (0.20 g), biotin (0.02 g), vitamin B-12 (2.50 g), vitamin E (15 g), vitamin A (0.80 g), vitamin D3 (0.25 g) and vitamin K (0.08 g).**

Table 3.2 Chemical composition of pelleted AIN-93G diets containing 45% kilocalories as fat and either non-fermentable dietary fiber or fructan prebiotics

Item	5% cellulose	10% cellulose	10% inulin	10% scFOS
DM, %	93.8	93.8	93.0	93.6
OM, %	96.0	96.2	96.2	96.2
Ash, %	4.1	3.9	3.8	3.9
CP, %	25.6	20.6	20.9	21.1
Acid hydrolyzed fat, %	25.2	24.1	23.8	22.3
Total dietary fiber, %	6.5	11.3	1.8	0.8
TDF calculated, %	6.4	11.2	12.8	11.8
Gross energy, kcal/g	5.6	5.4	5.4	4.8

Table 3.3 Villus height and crypt depth in the ileum, cecum, proximal colon, and distal colon of C57BL/6 mice (n=6)

	5% cellulose	10% cellulose	10% scFOS	10% inulin
Ileal villus height	201.0 ± 12.2^{b}	210.9 ± 12.2^{ab}	224.7 ± 12.2^{a}	204.0 ± 12.2^{ab}
Ileal crypt depth	90.9 ± 2.7^{c}	96.9 ± 2.7^{b}	123.0 ± 2.7^{a}	122.0 ± 2.7^{a}
Cecal crypt depth	109.3 ± 3.6^{b}	110.6 ± 3.6^{bc}	140.8 ± 3.6^{a}	110.6 ± 3.6^{a}
Proximal colon crypt depth	139.8 ± 11.3^{ab}	115.8 ± 11.3^{c}	126.8 ± 11.3^{b}	140.6 ± 11.3^{a}
Distal colon crypt depth	205.2 ± 7.7^{a}	211.5 ± 7.7^{a}	178.4 ± 7.7^{b}	205.3 ± 7.7^{a}

Values represents lsmeans ± pooled SEM. LSmeans lacking a common superscript letter differ ($p<0.05$).

Table 3.4 Contrasts between 5% cellulose and 10% cellulose treatments

	5% cellulose	10% cellulose	Pooled SEM
Villus : crypt ratio	2.1	1.9	0.1
All regions			
Crypt depth	135.7	144.3	2.6
Occludin mRNA abundance	1.2	0.9	0.1
Ileum			
Crypt depth	96.9	112.0	2.5
MUC2 mRNA abundance	0.7	0.4	0.1
Cecum			
Crypt depth	110.6	131.8	3.4
Proximal colon			
Crypt depth	115.8	135.7	10.9
Occludin mRNA abundance	1.6	0.8	0.1
AMPK mRNA abundance	1.5	1.2	0.2
Distal colon			
Crypt depth	211.5	196.3	7.2
Occludin mRNA abundance	1.2	0.7	0.1

All contrasts shown are significant ($p<0.05$).

Table 3.5 Contrasts between cellulose-containing treatments and fructan-containing treatments

	Cellulose fibers	Fructan fibers	Pooled SEM
Villus : crypt ratio	2.2	1.8	0.1
All regions			
Crypt depth	135.3	149.0	2.4
Transmural resistance	60.4	74.4	4.9
ZO-1 mRNA abundance	1.4	1.2	0.1
Occludin mRNA abundance	1.2	0.8	0.1
Ileum			
Crypt depth	93.9	122.5	2.5
MUC2 mRNA abundance	0.6	0.3	0.0
Occludin mRNA abundance	1.4	1.0	0.2
Cecum			
Crypt depth	110.0	143.0	3.2
Transmural Resistance	67.0	87.1	11.5
AMPK mRNA abundance	1.3	1.8	0.2
Occludin mRNA abundance	0.9	0.8	0.0
Proximal colon			
Crypt depth	127.8	133.7	10.8
MCT-1 mRNA abundance	0.8	0.5	0.1
ZO-1 mRNA abundance	1.3	1.0	0.1
AMPK mRNA abundance	1.4	1.1	0.1
Occludin mRNA abundance	1.4	0.7	0.1
Distal colon			
Crypt depth	208.3	191.9	7.0
Transmural Resistance	37.7	55.8	6.4
ZO-1 mRNA abundance	1.3	1.0	0.2
AMPK mRNA abundance	1.0	0.7	0.1
Occludin mRNA abundance	1.1	0.6	0.1

All contrasts shown are significant ($p<0.05$).

Table 3.6 Correlations between intestinal histomorphology, transmural resistance, and mRNA abundance in C57BL/6 mice

	Ileal villus height	Ileal crypt depth	Ileal transmural resistance	Cecal crypt depth	Cecal transmural resistance
MCT-1 (MCT-1 mRNA/18S rRNA)					
Ileum	-0.2	0.2	0.4		
Cecum				0.4	0.2
MUC2 (MUC2 mRNA/18S rRNA)					
Ileum	-0.5*	0.2	0.4*		
Cecum				0.0	0.1
Ocln (Occludin mRNA/18S rRNA)					
Ileum	0.1	0.2	0.4		
Cecum				0.1	0.2
		Proximal colon crypt depth	**Proximal colon transmural resistance**	**Distal colon crypt depth**	**Distal colon transmural resistance**
MUC2 (MUC2 mRNA/18S rRNA)					
Proximal colon		0.3	0.1		
Distal colon				-0.3	-0.2
AMPK (AMPK mRNA/18S rRNA)					
Proximal colon		0.5*	0.2		
Distal colon				0.3	0.4
ZO-1 (ZO-1 mRNA/18S rRNA)					
Proximal colon		0.5	-0.1		
Distal colon				0.0	0.6*

*p<0.05.

Table 3.7 Correlations between mRNA abundance in C57BL/6 mice

	MCT-1 (MCT-1 mRNA/18 rRNA) Ileum, cecum, proximal and distal colon	MCT-4 (MCT-4 mRNA/18 rRNA) Ileum, cecum, proximal and distal colon	AMPK (AMPK mRNA/18 rRNA) Ileum, cecum, proximal and distal colon	ZO-1 (ZO-1 mRNA/18 rRNA) Ileum, cecum, proximal and distal colon
AMPK (AMPK mRNA/18S rRNA)				
Ileum	0.4	0.2		
Cecum	0.3	0.3		
Proximal colon	0.4	-0.2		
Distal colon	0.6*	0.6*		
ZO-1 (ZO-1 mRNA/18S rRNA)				
Ileum	0.6*	0.2	0.9*	
Cecum	0.5*	0.4*	0.6*	
Proximal colon	0.2	0.1	0.7*	
Distal colon	0.8*	0.6*	0.8*	
Ocln (Occludin mRNA/18S rRNA)				
Ileum	0.0	-0.2	0.1	0.3
Cecum	0.1	0.3	0.0	-0.3
Proximal colon	0.1	- 0.3	0.4	0.5*
Distal colon	0.7*	0.3	0.7*	0.8*

*p<0.05.